

EARLINET correlative measurements for CALIPSO: First intercomparison results

Gelsomina Pappalardo,¹ Ulla Wandinger,² Lucia Mona,¹ Anja Hiebsch,² Ina Mattis,² Aldo Amodeo,¹ Albert Ansmann,² Patric Seifert,² Holger Linné,³ Arnoud Apituley,⁴ Lucas Alados Arboledas,⁵ Dimitris Balis,⁶ Anatoli Chaikovskiy,⁷ Giuseppe D'Amico,¹ Ferdinando De Tomasi,⁸ Volker Freudenthaler,⁹ Elina Giannakaki,⁶ Aldo Giunta,¹ Ivan Grigorov,¹⁰ Marco Iarlori,¹¹ Fabio Madonna,¹ Rodanthi-Elizabeth Mamouri,¹² Libera Nasti,¹³ Alexandros Papayannis,¹² Aleksander Pietruczuk,¹⁴ Manuel Pujadas,¹⁵ Vincenzo Rizi,¹¹ Francesc Rocadenbosch,¹⁶ Felicita Russo,¹ Franziska Schnell,⁹ Nicola Spinelli,¹³ Xuan Wang,^{13,17} and Matthias Wiegner⁹

Received 13 April 2009; revised 16 November 2009; accepted 24 November 2009; published 15 April 2010.

[1] A strategy for European Aerosol Research Lidar Network (EARLINET) correlative measurements for Cloud-Aerosol Lidar and Infrared Pathfinder Satellite Observation (CALIPSO) has been developed. These EARLINET correlative measurements started in June 2006 and are still in progress. Up to now, more than 4500 correlative files are available in the EARLINET database. Independent extinction and backscatter measurements carried out at high-performance EARLINET stations have been used for a quantitative comparison with CALIPSO level 1 data. Results demonstrate the good performance of CALIPSO and the absence of evident biases in the CALIPSO raw signals. The agreement is also good for the distribution of the differences for the attenuated backscatter at 532 nm ((CALIPSO-EARLINET)/EARLINET (%)), calculated in the 1–10 km altitude range, with a mean relative difference of 4.6%, a standard deviation of 50%, and a median value of 0.6%. A major Saharan dust outbreak lasting from 26 to 31 May 2008 has been used as a case study for showing first results in terms of comparison with CALIPSO level 2 data. A statistical analysis of dust properties, in terms of intensive optical properties (lidar ratios, Ångström exponents, and color ratios), has been performed for this observational period. We obtained typical lidar ratios of the dust event of 49 ± 10 sr and 56 ± 7 sr at 355 and 532 nm, respectively. The extinction-related and backscatter-related Ångström exponents were on the order of 0.15–0.17, which corresponds to respective color ratios of 0.91–0.95. This dust event has been used to show the methodology used for the investigation of spatial and temporal representativeness of measurements with polar-orbiting satellites.

Citation: Pappalardo, G., et al. (2010), EARLINET correlative measurements for CALIPSO: First intercomparison results, *J. Geophys. Res.*, 115, D00H19, doi:10.1029/2009JD012147.

¹Istituto di Metodologie per l'Analisi Ambientale, IMAA, CNR, Potenza, Italy.

²Leibniz-Institut für Troposphärenforschung, Leipzig, Germany.

³Max-Planck-Institut für Meteorologie, Hamburg, Germany.

⁴Rijksinstituut voor Volksgezondheid en Milieu, Bilthoven, Netherlands.

⁵Universidad de Granada, Granada, Spain.

⁶Aristotle University of Thessaloniki, Thessaloniki, Greece.

⁷Institute of Physics, National Academy of Sciences, Minsk, Belarus.

⁸Department of Physics, Università del Salento, Lecce, Italy.

⁹Ludwig-Maximilians-Universität, Munich, Germany.

¹⁰Institute of Electronics, Bulgarian Academy of Sciences, Sofia, Bulgaria.

¹¹CETEMPS, Dipartimento di Fisica, Università degli Studi dell'Aquila, L'Aquila, Italy.

¹²Department of Physics, National Technical University of Athens, Athens, Greece.

¹³Consorzio Nazionale Interuniversitario per le Scienze Fisiche della Materia, Naples, Italy.

¹⁴Institute of Geophysics, Polish Academy of Sciences, Warsaw, Poland.

¹⁵Centro de Investigaciones Energéticas, Medioambientales y Tecnológicas, Madrid, Spain.

¹⁶IEEC, CRAE, Universitat Politècnica de Catalunya, Barcelona, Spain.

¹⁷Coherentia, INFN, CNR, Naples, Italy.

1. Introduction

[2] The knowledge about aerosol radiative forcing and the resulting impact on climate will be significantly improved by measurements obtained with a new generation of satellite-borne aerosol lidar instruments providing aerosol vertical profiles. It is well known that the high variability of tropospheric aerosols both in space and time is one of the main reasons of the high uncertainty of radiative forcing estimates in studies of future climate change [Forster et al., 2007]. In the past, global aerosol distribution and optical properties were investigated by means of passive remote sensing instruments aboard satellites or ground-based Sun photometer networks like AERONET [Holben et al., 1998; Kaufman et al., 2000; Omar et al., 2005; Kahn et al., 2007]. However, these instruments cannot provide information about the vertical layering of aerosol. The aerosol vertical distribution is of crucial importance in radiative transfer calculations and in the study of aerosol-cloud interaction. The not well understood vertical mixing of aerosols also significantly contributes to the aerosol variability, but is typically not considered in models. Vertical mixing can lead to significant horizontal inhomogeneities and influences the lifetime of aerosol. Lofted aerosol layers in the free troposphere travel over large distances and can even be hemispherically distributed [e.g., Forster et al., 2001; Damoah et al., 2004; Mattis et al., 2003; Müller et al., 2007a; Mattis et al., 2008].

[3] In studying the vertical structure of the aerosol field and its temporal and spatial evolution, lidar techniques represent an indispensable tool because of their capability to provide aerosol profiles with high resolution both in time and in horizontal and vertical dimension. Furthermore, lidar techniques allow an aerosol-cloud separation and the penetration of optically thin clouds and, therefore, the investigation of aerosol-cloud interactions, information strongly needed for studying aerosol indirect effects on the radiation budget.

[4] In this context, the Cloud-Aerosol Lidar and Infrared Pathfinder Satellite Observations (CALIPSO) mission provides a unique opportunity to address the four-dimensional distribution of aerosols and clouds on a global scale. Cloud-Aerosol Lidar with Orthogonal Polarization (CALIOP) is the first satellite-borne lidar specifically designed for aerosol and cloud observation. Before that, the first well-documented experience with lidar in space was the Lidar In-space Technology Experiment (LITE) mission, an 11 day mission on the space shuttle carried out in 1994 [McCormick et al., 1993; Ansmann et al., 1997]. Although it was a very short time experience, LITE provided for the first time a snapshot of the atmospheric layering on large scales and paved the way for the current and future spaceborne lidar missions. Since its first light in May 2006, CALIPSO has delivered high-vertical-resolution profiles of aerosols and clouds on the global scale [Winker et al., 2007].

[5] In order to increase and validate the accuracy of aerosol optical properties retrieved from CALIPSO's pure backscatter lidar data, comparison with ground-based lidar observations is required. Because of its geographic coverage and the deployment of advanced Raman aerosol lidars, European Aerosol Research Lidar Network (EARLINET) offers a unique opportunity for the validation and full exploitation of the CALIPSO mission. EARLINET provides

long-term, quality-assured aerosol data and, because of its geographical distribution over Europe, allows us to investigate a large variety of different aerosol situations with respect to layering, aerosol type, mixing state, and properties in the free troposphere and the local planetary boundary layer [e.g., Ansmann et al. 2003; Matthias et al., 2004; Mattis et al., 2004, 2008; Pappalardo et al., 2004a; Mona et al., 2006; Balis et al., 2003; Wandinger et al., 2004; Amiridis et al., 2005; De Tomasi et al., 2006; Wiegner et al., 2006; Papayannis et al., 2005, 2008]. With a network on a continental scale it also becomes possible to study the representativeness of the limited number of satellite lidar cross sections along an orbit against long-term network observations.

[6] A further aspect of EARLINET's space-related activities is the provision of a long-term ground-based support of spaceborne lidar missions in order to homogenize data sets obtained with different instruments on different platforms. The CALIPSO launch date is regarded the starting point of long-lasting, global, four-dimensional observations that will substantially improve our knowledge on the role of aerosols and clouds in the Earth's climate system. The Atmospheric Dynamics Mission-Aeolus of the European Space Agency ESA (ADM-Aeolus) [Stoffelen et al., 2005; Ansmann et al., 2007] and Earth Clouds, Aerosols and Radiation Explorer (EarthCARE) of ESA and the Japan Aerospace Exploration Agency JAXA [Hélière et al., 2008] missions will continue such kind of measurements in subsequent years and extend the data set to more than a decade of observations. However, the lidar instruments onboard the three missions represent different system types with different sets of measured parameters at different wavelengths (ADM, EarthCARE, 355 nm; CALIPSO 532 and 1064 nm). In order to establish a homogeneous aerosol and cloud data set from spaceborne observations, long-term ground-based support with advanced multiwavelength lidar instruments is required. The ground-based instruments must deliver wavelength conversion information for different aerosol and cloud types to relate the spaceborne measurements at 355, 532, and 1064 nm to each other. EARLINET comprises a number of sophisticated multiwavelength lidar instruments and is therefore an optimum tool in this context. EARLINET started correlative measurements for CALIPSO on 14 June 2006, i.e., at the beginning of the CALIPSO operation. A strategy for correlative measurements has been defined on the base of the analysis of the ground track data provided by NASA. While the majority of EARLINET stations contributed on a voluntary basis to this measurement program in the first two years of the mission, a dedicated ESA activity supports correlative EARLINET-CALIPSO observations at 16 selected EARLINET stations since 1 April 2008. Data exploitation within this study aims at a long-term aerosol and cloud database providing type-dependent wavelength conversion factors as well as EARLINET-CALIPSO intercomparison data based on level 2 profile and layer products.

[7] In this paper the general approach for the EARLINET correlative study for CALIPSO is presented. Specific examples are discussed in order to present this statistical approach for validation purposes, for both measured CALIPSO level 1 data and retrieved CALIPSO level 2 data, and for representativeness studies. The paper starts with an overview of EARLINET (section 2) and in particular of the

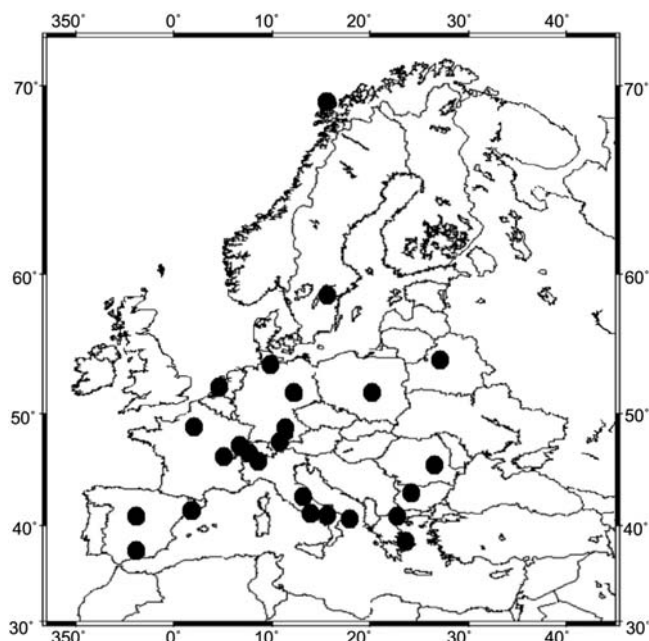


Figure 1. Map of Europe with the distribution of all the EARLINET lidar stations.

EARLINET correlative measurements for CALIPSO regarding both the observation and the validation strategy (section 3). First intercomparison results with CALIPSO level 1 data are presented and discussed in section 4. For an episode of high Saharan dust load over Europe in May 2008, we also discuss level 2 data intercomparisons and issues of spatial and temporal inhomogeneity. We describe the idea of the long-term database of correlative ground-based and spaceborne observations and illustrate the potential of the lidar network to provide a sustainable ground-based support for spaceborne lidar missions. In section 5, the methodology used for the investigation of spatial and temporal representativeness of measurements with polar-orbiting satellites is presented together with examples. Section 6 summarizes the paper.

2. EARLINET

[8] EARLINET is the first coordinated aerosol lidar network, established in 2000, with the main goal to provide a comprehensive, quantitative, and statistically significant database for the aerosol distribution on a continental scale [Bösenberg *et al.*, 2003]. At present, the network includes 25 stations distributed over Europe (Figure 1): 10 single-backscatter lidar stations, 8 Raman lidar stations with the UV Raman channel for independent measurements of aerosol extinction and backscatter, and 7 multiwavelength Raman lidar stations (elastic channels at 1064 nm, 532 nm, 355 nm, Raman channels at 532 nm and 355 nm, plus depolarization channel at 532 nm). The wavelength dependence of the backscatter and extinction coefficients and of the respective extinction-to-backscatter ratios (lidar ratios) allows for a more detailed discrimination of aerosol types. In the framework of EARLINET, inversion algorithms were developed to obtain microphysical aerosol properties like effective radius, volume and surface area concentration, and real and imagi-

nary part of the complex refractive index from multiwavelength Raman lidar data. Backscatter coefficients at three wavelengths plus extinction coefficients at two wavelengths (so-called 3 + 2 measurements) are the minimum required input data for such inversion schemes [Müller *et al.*, 2001; Veselovskii *et al.*, 2002; Böckmann *et al.*, 2005; Ansmann and Müller, 2005]. Locations of EARLINET lidar stations and measured aerosol parameters are reported in Table 1.

[9] Lidar observations within the network are performed on a regular schedule of one daytime measurement per week around noon, when the boundary layer is usually well developed, and two nighttime measurements per week, with low background light, in order to perform Raman extinction measurements. This data set is used to obtain unbiased data for climatological studies. In addition to the routine measurements, further observations are devoted to monitor special events such as Saharan dust outbreaks [Ansmann *et al.*, 2003; Papayannis *et al.*, 2008], forest fires [Mattis *et al.*, 2003; Müller *et al.*, 2007b], photochemical smog, and volcano eruptions [Pappalardo *et al.*, 2004a].

[10] Data quality has been assured by intercomparisons at instrument level using the available transportable systems [Matthias *et al.*, 2004]. The quality assurance also included the intercomparison of the retrieval algorithms for both backscatter and Raman lidar data [Böckmann *et al.*, 2004; Pappalardo *et al.*, 2004b]. The data quality control establishes a common European standard for routine quality assurance of lidar instruments and algorithms and ensures the data products provided by the individual stations are homogeneous and permanently of highest possible quality according to common standards. Efforts to guarantee high-quality observations are ongoing [e.g., Freudenthaler, 2008].

[11] EARLINET measurements are performed since 1 May 2000. All measured profiles are stored in a standardized data format in a centralized database which allows for an easy access to the complete data set for further scientific studies. Up to now the EARLINET database represents the largest database for the aerosol distribution on a continental scale. All the aerosol profile data files are divided in different categories related to regular measurements and special conditions: (1) climatology (regular measurements); (2) cirrus; (3) diurnal cycles (diurnal and seasonal cycle of aerosols in the boundary layer); (4) volcanic eruptions (observations of the Etna eruption events in 2001 and 2002); (5) forest fires (observations of large forest fires); (6) photosmog (observations of photochemical smog episodes in large cities); (7) rural/urban (nearly simultaneous measurements at pairs of stations that are sufficiently close to minimize the effect of large-scale patterns, but sufficiently apart to reflect the differences in the surrounding: urban versus rural or prerural); (8) Saharan dust (special observations of Saharan dust outbreaks using dust forecast); (9) stratosphere (stratospheric aerosol observations and detection of smaller-scale features of stratospheric aerosol distribution and its interdependence with dynamics and heterogeneous chemistry); and (10) CALIPSO (correlative measurements in coincidence of the CALIPSO overpasses).

[12] In particular, the EARLINET database contains a large data set of the aerosol lidar ratio retrieved from simultaneous and independent lidar measurements of aerosol extinction and backscatter coefficients. This is by far the

Table 1. Locations of EARLINET Lidar Stations, Corresponding Identification Codes, Altitude, Geographical Coordinates, and Corresponding Measurable Aerosol Parameters^a

| Site | Identification Code | Altitude asl (m) | Latitude (°N) | Longitude (°E) | Data Products Available |
|--|---------------------|------------------|---------------|----------------|---|
| Andøya, Norway | an | 380 | 69.28 | 16.01 | aerosol height/thickness, β (355), τ (355), σ (355), S (355), β (532), τ (532), σ (532), S (532), β (1064), water vapor mixing ratio |
| Athens, Greece | at | 200 | 37.96 | 23.78 | aerosol height/thickness, β (355), τ (355), σ (355), S (355), β (532), τ (532), σ (532), S (532), β (1064), water vapor mixing ratio |
| Barcelona, Spain | ba | 115 | 41.39 | 2.11 | aerosol height/thickness, β (532), τ (532), σ (532), S (532), β (1064) |
| Belsk, Poland | be | 180 | 51.84 | 20.79 | aerosol height/thickness β (532), β (1064) |
| Bucharest-Magurele, Romania | bu | 93 | 44.45 | 26.03 | aerosol height/thickness, β (355), τ (355), σ (355), S (355), β (532), τ (532), σ (532), S (532), β (1064), $\beta'(R, 532)_{\parallel}/\beta'(R, 532)_{\perp}$, water vapor mixing ratio |
| Cabauw, Netherlands | ca | 1 | 51.97 | 4.93 | aerosol height/thickness, β (355), τ (355), σ (355), S (355), β (532), τ (532), σ (532), S (532), β (1064), water vapor mixing ratio |
| Garmisch-Partenkirchen, Germany | gp | 730 | 47.48 | 11.06 | aerosol height/thickness, β (532), τ (532), σ (532), S (532), β (355), β (1064), extinction 532 at daytime |
| Granada, Spain | gr | 680 | 37.16 | -3.61 | aerosol height/thickness, β (532), τ (532), σ (532), S (532), β (1064), β (355), τ (355), σ (355), S (355), $\beta'(R, 532)_{\parallel}/\beta'(R, 532)_{\perp}$, water vapor mixing ratio |
| Hamburg, Germany | hh | 25 | 53.57 | 9.97 | aerosol height/thickness, β (355), τ (355), σ (355), S (355), β (532), τ (532), σ (532), S (532), β (1064), $\beta'(R, 532)_{\parallel}/\beta'(R, 532)_{\perp}$, water vapor, temperature |
| Ispira, Italy | is | 209 | 45.82 | 8.63 | aerosol height/thickness, β (532) |
| L'Aquila, Italy | la | 683 | 42.38 | 13.32 | aerosol height/thickness, β (355), τ (355), σ (355), S (355), $\beta'(R, 355)_{\parallel}/\beta'(R, 355)_{\perp}$, water vapor and cloud liquid water profiles. |
| Lecce, Italy | lc | 30 | 40.30 | 18.10 | aerosol height/thickness, β (355), τ (355), σ (355), S (355), $\beta'(R, 355)_{\parallel}/\beta'(R, 355)_{\perp}$, water vapor mixing ratio profiles at nighttime |
| Leipzig, Germany | le | 100 | 51.35 | 12.44 | aerosol height/thickness, τ (355), σ (355), β (355), S (355), τ (532), σ (532), β (532), S (532), $\beta'(R, 532)_{\parallel}/\beta'(R, 532)_{\perp}$, β (1064) |
| Linköping, Sweden | lk | 80 | 58.39 | 15.57 | water vapor mixing ratio, temperature |
| Madrid, Spain | ma | 669 | 40.45 | -3.73 | aerosol height/thickness, τ (355), σ (355), β (355), S (355), τ (532), σ (532), β (532), S (532), aerosol height/thickness, |
| Maisach, Germany | ms | 515 | 48.21 | 11.26 | τ (532), σ (532), β (532), S (532), aerosol height/thickness, β (532), τ (532), σ (532), S (532), β (1064), β (355), τ (355), σ (355), S (355), $\beta'(R, 532)_{\parallel}/\beta'(R, 532)_{\perp}$ |
| Minsk, Belarus | mi | 200 | 53.92 | 27.60 | aerosol height/thickness, β (532), β (1064), β (355), τ (355), σ (355), S (355), $\beta'(R, 532)_{\parallel}/\beta'(R, 532)_{\perp}$ |
| Napoli, Italy | na | 118 | 40.84 | 14.18 | aerosol height/thickness, β (532), τ (532), σ (532), S (532), β (355), τ (355), σ (355), S (355), water vapor mixing ratio |
| Neuchâtel, Switzerland | ne | 487 | 47.00 | 6.96 | aerosol height/thickness, β (532), $\beta'(R, 532)_{\parallel}/\beta'(R, 532)_{\perp}$ |
| Observatoire de Haute-Provence, France | hp | 683 | 43.96 | 5.71 | aerosol height/thickness, β (532) |
| Palaiseau, France | pl | 162 | 48.70 | 2.20 | aerosol height/thickness, β (532), β (1064), $\beta'(R, 532)_{\parallel}/\beta'(R, 532)_{\perp}$ |
| Payerne, Switzerland | py | 456 | 46.81 | 6.94 | aerosol height/thickness, τ (355), σ (355), β (355), S (355), water vapor mixing ratio |

Table 1. (continued)

| Site | Identification Code | Altitude asl (m) | Latitude (°N) | Longitude (°E) | Data Products Available |
|---------------------------|---------------------|------------------|---------------|----------------|--|
| Potenza-Tito Scalo, Italy | po | 760 | 40.60 | 15.72 | aerosol height/thickness, β (355), τ (355), σ (355), S (355), β (532), τ (532), σ (532), S (532), β (1064), β'_{\parallel} (R, 532)/ β'_{\perp} (R, 532) _L , water vapor mixing ratio |
| Sofia, Bulgaria | sf | 550 | 42.67 | 23.33 | aerosol height/thickness, β (511) |
| Thessaloniki, Greece | th | 60 | 40.63 | 22.95 | aerosol height/thickness, β (355), τ (355), σ (355), S (355), β (532), τ (532), σ (532), S (532) |

^aAbbreviations: β , backscatter coefficient profile; σ , extinction coefficient profile; τ , optical depth (columnar quantity); S, lidar ratio profile; β'_{\parallel} and β'_{\perp} , parallel polarized and cross polarized components, respectively, of radiation.

largest data set of lidar ratio data on a continental scale covering about 10 years of systematic observations. The lidar ratio is a very important parameter for the characterization of the aerosol and is of fundamental importance for the estimation of aerosol extinction from pure backscatter lidar measurements such as conducted with CALIPSO [Winker *et al.*, 2004]. This latter issue makes the EARLINET observations especially valuable.

3. EARLINET Correlative Measurements for CALIPSO

[13] Already before the launch of CALIPSO, a strategy for correlative measurements had been developed within EARLINET. Based on the experience of the first 18 months of correlative observations we have consolidated this strategy in the frame of a dedicated ESA study aiming at a long-term aerosol and cloud database from ground-based and satellite-borne lidars which started on 1 April 2008. The main goal is to obtain a statistically significant data set from network observations with ground-based lidars to correlate it to CALIPSO observations for validation purposes and also for a possible use of integrated lidar measurements from satellite and from ground for studying aerosol and cloud variability in space and time. To achieve this goal, a large record of CALIPSO-EARLINET correlative measurements has to be sampled.

[14] Furthermore, these measurements should allow the investigation of aerosol and cloud properties as a function of geographical region. This will be important for investigations of representativeness and for the derivation of intensive aerosol optical properties for regions with different characteristics in terms of orography and aerosol type.

[15] Finally, a representativeness study should take into account the variability of aerosol and cloud fields. This is particularly true when a single ground-based measurement is compared to a single satellite-borne measurement with a given horizontal distance between the two sampled air volumes and different signal averaging periods (observational time intervals). Therefore, the strategy for EARLINET-CALIPSO correlative measurements should attempt to address also this point and try to quantify this variability.

[16] The EARLINET-CALIPSO correlative measurement plan considers the criteria established in the CALIPSO validation plan (<http://calipsovalidation.hamptonu.edu>). In particular, EARLINET participating stations have to perform measurements, as close in time as possible, when

CALIPSO overpasses their location within a horizontal radius of 100 km. These measurements are called case A measurements and allow the point-to-point comparison between ground-based and satellite-borne lidar measurements. In this kind of comparison, the atmospheric variability both in time and space is a fundamental point. In this sense it is important to define how long a correlative measurement should last.

[17] Besides source and formation mechanisms of both aerosol and cloud features, wind is of course one of the main factors driving the variability. Annual mean wind speed profiles at EARLINET stations show typical values between 5 and 20 m/s in the free troposphere. CALIPSO aerosol retrievals are performed at 5, 20 or 80 km horizontal resolution and level 2 profiles (version 2.01) are provided at a fixed horizontal resolution of 40 km. Therefore, in order to investigate comparable length scales, an integration time for EARLINET measurements of about 30–130 min has to be considered. It follows that to investigate the temporal variability of aerosol/cloud fields, a temporal window of observations lasting for 150 min (centered around the overpass) is needed for each EARLINET correlative measurement whenever atmospheric conditions allow it.

[18] For the dedicated activities within the frame of the ESA-EARLINET-CALIPSO project, we have defined two types of stations: high-performance and contributing stations. High-performance stations are equipped with instruments which measure at least extinction and backscatter coefficients at both 355 and 532 nm (two-wavelength Raman lidar). Most of these stations provide backscatter coefficients at 1064 nm and the depolarization ratio at 532 nm as well (see, e.g., Ansmann and Müller [2005] for a general description of aerosol retrieval methods). Their measurements can be used to estimate important microphysical particle properties like parameters of the size distribution, refractive index, and derived quantities such as particle mass and surface area concentration or single-scattering albedo. This detailed information from the EARLINET core stations offers the unique chance to investigate the potential of spaceborne lidar instruments to identify certain aerosol types and to distinguish man-made from natural aerosol. The data can be used to develop a highly sophisticated classification scheme for aerosol type considering the CALIOP as well as the ALADIN (ADM-Aeolus lidar) and ATLID (EarthCARE lidar) data information content.

[19] The stations are located such that four European core regions are covered (see Figure 2): central Europe (Germany

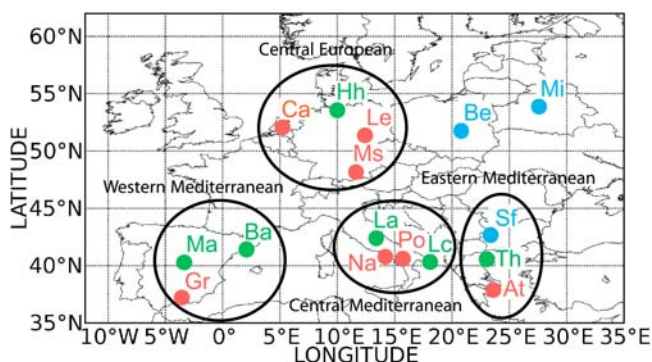


Figure 2. Identified clusters within EARLINET. High-performance stations are reported as red dots, green dots represent contributing Raman lidar stations, and blue dots indicate contributing elastic-backscatter lidar stations.

and Netherlands), the western Mediterranean (Spain), the central Mediterranean (Italy), and the eastern Mediterranean (Greece). In this way, a broad variety of aerosol types and scenarios can be investigated, which include maritime aerosols (Cabauw), urban aerosols (Leipzig, Napoli), rural aerosols (Maisach, Potenza), fresh Saharan dust (Mediterranean stations), aged Saharan dust (all stations), fresh forest fire smoke (Mediterranean stations), aged forest fire aerosols (central European stations), photochemical smog (Athens), and long-range-transport aerosol in the free troposphere from America and Asia (all stations).

[20] The selected contributing stations create clusters around the high-performance stations (see Figure 2). All these stations operate Raman lidar instruments as well, but not at several wavelengths. Highly reliable extinction and backscatter coefficients are retrieved at either 355 or 532 nm at these sites. Typical distances of neighboring stations within a cluster are 120 to about 800 km. The distribution of the stations allows us to study the temporal, regional and continental-scale representativeness of the observations and to compare these findings with the results of spaceborne lidar measurements from the polar-orbiting satellites. The stations in Belsk, Minsk, and Sofia operate backscatter lidars, in case of Belsk and Minsk at multiple wavelengths. These stations were chosen for the study because they extend the network to eastern Europe and can provide valuable information on aerosol source regions. It has been found that pollution from eastern and southeastern Europe, especially from the Black Sea area, can have a substantial influence on the aerosol load over central Europe and the eastern Mediterranean [Wandinger *et al.*, 2004].

[21] Keeping these facts in mind, the observation strategy schedules additional contemporary measurements at several EARLINET stations of the same cluster, called case B measurements. Also for the case B measurements, 150 min records of measurements (centered around the overpass) are requested, in order to investigate the temporal variability. For each recurring 16 day cycle of CALIPSO observations, two measurements involving two or more EARLINET stations are performed for each cluster in daytime conditions. In nighttime conditions, three measurements involving two or more stations are scheduled for the central European,

western Mediterranean and central Mediterranean clusters and two measurements for the eastern Mediterranean cluster and for Belsk and Minsk.

[22] Further observations, called case C measurements, are performed in conjunction with special events like Saharan dust outbreaks and forest fire events. The collection of these measurements allows us to study specific aerosol types and their optical properties in more detail and to investigate regional and continental-scale representativeness of the observations. In synthesis, the EARLINET observation strategy foresees these measurements: (1) case A (CALIPSO overpass within 100 km); (2) case B (more than one station of the same cluster perform contemporary measurements); and (3) case C (interesting additional cases like Saharan dust intrusions, forest fires etc.).

[23] Starting from the high-resolution ground track data provided by NASA, the time schedule of case A and case B measurements is calculated for all participating stations, with exact distance between EARLINET stations and CALIPSO ground track and time of the CALIPSO overpass. This schedule is updated and distributed weekly to the whole network. Besides case A and case B measurements, which can be scheduled in advance, case C measurements are requested for special events. For these measurements, a devoted e-mail alert system has been established within EARLINET at both central and cluster level.

[24] After about 2.5 years since the beginning of correlative observations on 14 June 2006, more than 6500 h of correlative measurements have been performed and about 3100 correlative files have been uploaded into the EARLINET database in the CALIPSO category.

[25] A number of modeling tools is used for the aerosol type and source identification in addition to the information derived from the multiwavelength lidar observations. The German Meteorological Service (DWD) provides 4 day backward trajectories on a daily schedule for all EARLINET stations for 6 arrival heights between 925 and 200 hPa and for 2 arrival times (1300 UTC and 1900 UTC). The Dust REgional Atmospheric Model (DREAM) [Nickovic *et al.*, 2001] is used for the coordination of intensive measurement periods during dust outbreaks over Europe. The Barcelona Supercomputing Center provides daily updated analysis data and dust forecasts up to 72 h. DREAM is also applied to predict vertical profiles of the dust concentration at 20 EARLINET sites. The Lagrangian particle dispersion model FLEXPART [Stohl *et al.*, 1998; Stohl and Thomson, 1999] has been implemented for EARLINET at the Leipzig station to study aerosol origin, transport, and mixing. FLEXPART is combined with aerosol source information from European Monitoring and Evaluation Programme (EMEP) emission inventories to account for anthropogenic emissions from industry and traffic. Smoke sources are identified using the fire maps produced from data of the Moderate Resolution Imaging Spectroradiometer (MODIS).

4. EARLINET-CALIPSO Correlative Studies

4.1. CALIPSO Data

[26] CALIPSO data are classified in level 1 and level 2 products. A complete overview of the CALIPSO mission and CALIOP data products is given by Winker *et al.* [2009].

CAL_LID_L1-Prov-V2-01 data are available for the period starting from 13 June 2006 to 13 September 2008, while a different release, namely, V2-02 is available for data acquired after 14 September 2008 to February 2009. More detailed information about these data sets can be found in the CALIOP Algorithm Theoretical Basis Documents, Calibration and level 1 Data products, available at <http://eosweb.larc.nasa.gov> (PC-SCI-201). The main level 1 CALIPSO data products are the vertical profiles of the so-called attenuated backscatter. From the CALIPSO point of view, the attenuated backscatter is the calibrated lidar range-corrected signal, obtained after the subtraction of the background.

[27] Level 2 CALIPSO data provide geophysical products. In particular, two different kinds of level 2 data are provided: level 2 layer data and level 2 profile data. Level 2 layer products are the optical and geometrical properties of identified atmospheric layers. Four different level 2 layer files are produced for each observation: three for clouds at different horizontal resolutions (333 m, 1 km and 5 km) and one for aerosol at 5 km horizontal resolution. The layer identification is performed by means of a complex algorithm that is mainly based on a threshold routine, in which the threshold is altitude-dependent. A special procedure is used to avoid false alarms due to noise and of course clouds are handled differently from aerosols. For each of the layers, integrated attenuated backscatter at 532 and 1064 nm, the integrated volume depolarization ratio and the integrated attenuated color ratio (i.e., the ratio between attenuated backscatter at 1064 nm and 532 nm) are reported. For each of these quantities, their statistical values (mean, std, min, max, centroid, skewness) are also stored.

[28] In addition to these quantities, level 2 layer data report also the feature classification flag that provides information about the feature type (e.g., cloud versus aerosol versus stratospheric layer), feature subtype (kind of aerosol), layer ice water phase (clouds only), and the amount of horizontal averaging required for layer detection. The cloud-aerosol discrimination (CAD) score provides information about the results obtained for each layer by the CALIOP-CAD algorithm. The CAD algorithm separates clouds and aerosols based on multidimensional, altitude-dependent histograms of scattering properties (e.g., intensity and spectral dependence).

[29] As in level 1 data, level 2 data are actually available in two different versions, V2-01 for data acquired before 14 September 2008 and version V2-02 for the following period. More detailed information about these data sets is available in the documentation downloadable at <http://eosweb.larc.nasa.gov> (PC-SCI-202).

[30] For the EARLINET-CALIPSO correlative study, a specific subset of CALIPSO data related to Europe and surrounding areas is considered as fundamental. This subset (namely 20°N–80°N, 20°W–50°E) has been extracted from the original CALIPSO database by NASA and has been provided directly to EARLINET.

4.2. EARLINET Comparisons With CALIPSO Level 1 Data

[31] Ground-based 3 + 2 lidar measurements (providing, as mentioned, backscatter coefficients at three wavelengths and extinction coefficients at two wavelengths) are an optimal tool for validation of CALIPSO products. The

EARLINET 3 + 2 systems provide independent measurements of the particle backscatter and extinction profiles at 532 nm and backscatter profiles at 1064 nm that can be directly compared to respective quantities derived from CALIPSO. However, before these comparisons can be made, it is necessary to assess the quality of CALIPSO level 1 data in order to distinguish problems and possible biases contained in the acquired lidar signal, mainly due to calibration uncertainties and possible calibration biases [Powell *et al.*, 2009], from uncertainties and errors related to the retrieval algorithms.

[32] For this comparison we selected the EARLINET stations providing independent extinction profiles at 532 nm. The attenuated backscatter profiles as measured with CALIPSO are not directly comparable to ground-based EARLINET profiles, because the ground-based stations operate upward looking lidars and CALIOP is a downward looking lidar. A specific procedure has to be followed in order to compare these independent measurements. This procedure is discussed in detail by *Mona et al.* [2009] where it is shown that starting from simultaneous and independent measurements of aerosol backscatter and extinction profiles measured by EARLINET, it is possible to calculate the CALIPSO-like attenuated backscatter (CLAB) profile at 532 nm without any assumptions.

[33] For a quantitative comparison between ground-based and CALIPSO lidar data in terms of attenuated backscatter, we selected nighttime cases from all EARLINET case A measurements, because in the absence of solar background it is possible to obtain independent measurements of backscatter and extinction coefficient profiles with the EARLINET Raman lidars. The number of possible comparisons is limited by some constraints. First of all, it has to be considered that on average there are 2–3 CALIPSO overpasses for each station every month during nighttime, when Raman measurements are possible. Second, measurements at ground-based stations are not performed in presence of low clouds or, more generally, under bad weather conditions. Hence, typically only 50% of the scheduled measurements are performed, even if this percentage changes with the location and orography. Finally, it may happen that suitable measurements have been performed at ground-based stations but EARLINET and/or CALIPSO corresponding profiles are not available on the respective databases at the time of the data analysis. Cases with presence of cirrus clouds detected in EARLINET and/or CALIPSO measurements are not considered for this comparison because the horizontal variability in cirrus clouds is too large for a comparison of lidar systems with several tens of kilometers horizontal distance. In addition, in presence of cirrus clouds, multiple scattering is typically not negligible, in particular for spaceborne lidars [Winker, 2003]. The main effect of multiple scattering is an apparent extinction and optical depth lower than the real one, with an almost unchanged backscatter. For CALIPSO data, the multiple-scattering influence on level 1 data has been observed through the comparison with collocated AIRS data [Lamquin *et al.*, 2008]. Furthermore, it is well known that lidar measurements of ice clouds are typically affected by specular reflections, when the lidar is pointing at zenith or nadir [Young and Vaughan, 2009]. Specular reflections cause anomalously high backscatter, without any increase in the extinction [Ansmann *et al.*, 1992; Seifert *et*

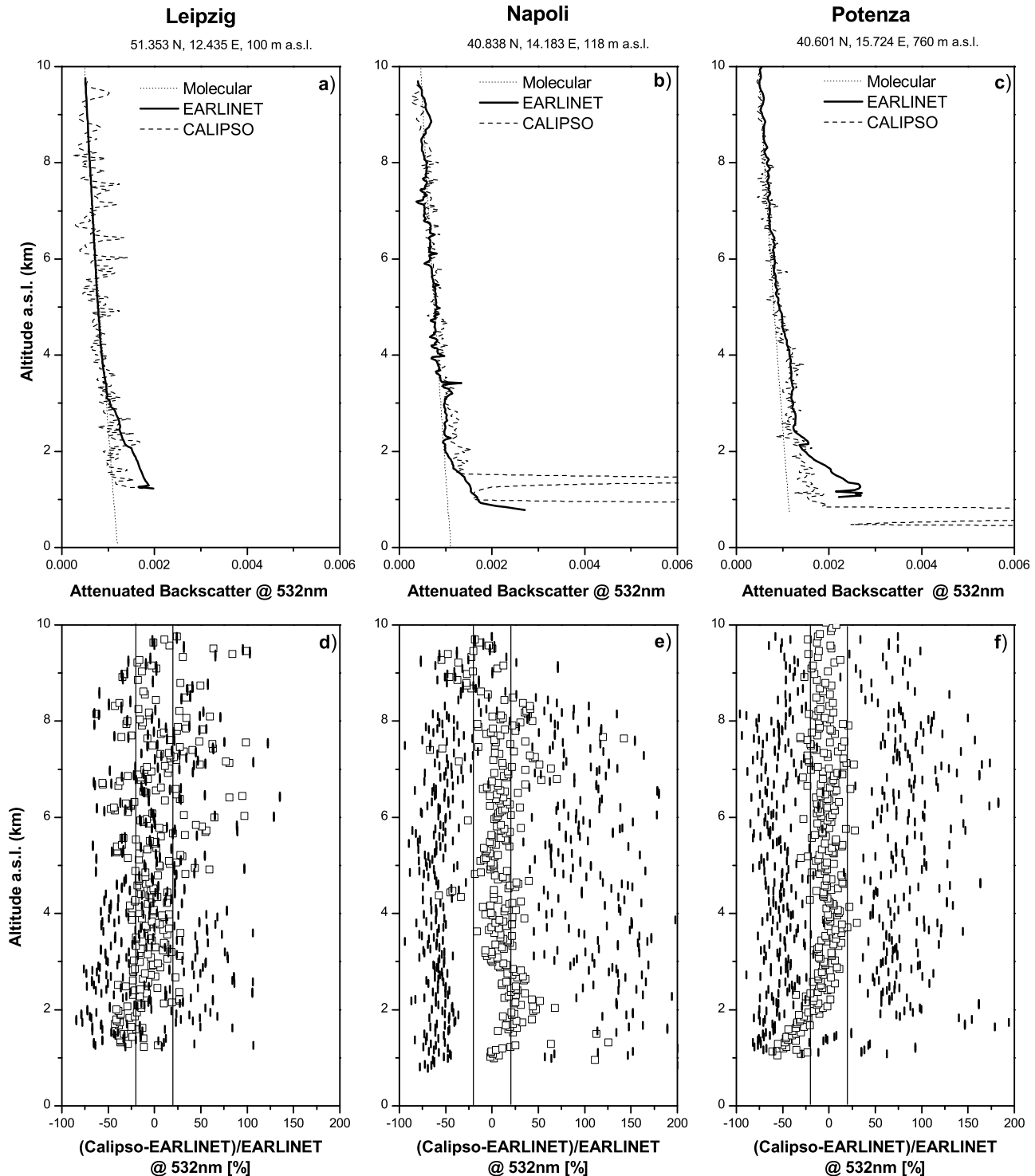


Figure 3. CALIPSO (dashed line) and EARLINET (solid line) mean profiles of attenuated backscatter at 532 nm for the (a) Leipzig, (b) Napoli, and (c) Potenza stations. Mean profiles of attenuated backscatter have been calculated over 4, 21, and 11 available cases for Leipzig, Napoli, and Potenza, respectively. The molecular attenuated backscatter profiles, including ozone contribution, are reported as dotted lines. Mean percentage difference between CALIPSO and EARLINET attenuated backscatter measured at 532 nm (open squares) reported as a function of the altitude for the (d) Leipzig, (e) Napoli, and (f) Potenza stations. The maximum and minimum values are reported, too, as indication of the variability (black vertical bars). Vertical solid lines limit the region within 20% as difference.

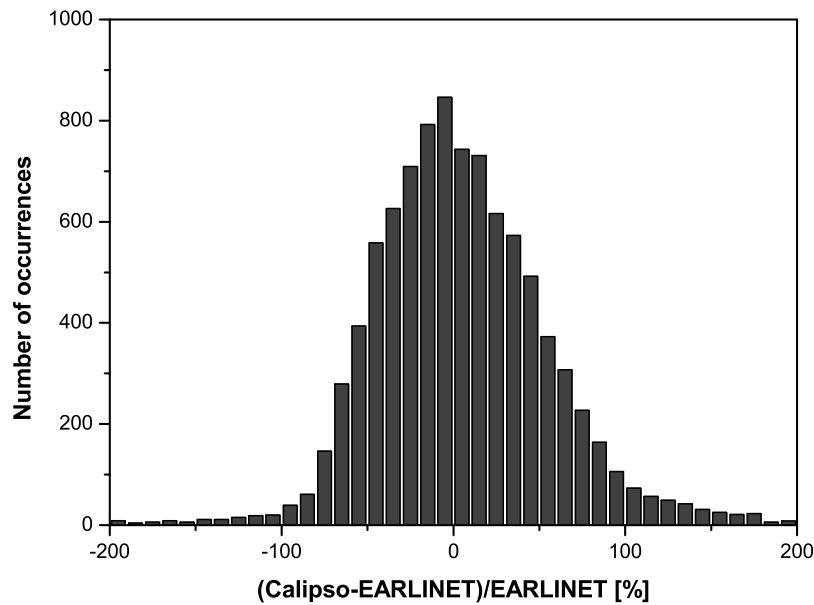


Figure 4. Distribution of the mean relative differences between CALIPSO level 1 and corresponding EARLINET attenuated backscatter measurements. The calculation has been performed using data provided by the 3 + 2 stations of Leipzig, Napoli, Potenza, Madrid, and Barcelona.

al., 2008]. CALIOP was nominally pointing in ‘near nadir’ direction ($\sim 0.3^\circ$ off nadir) until 28 November 2007, and therefore specular reflection effects cannot be neglected a priori. The same holds for most of the EARLINET lidars which typically point at zenith.

[34] Considering these well-known effects, only cases without cirrus clouds both in EARLINET and CALIPSO data are used for this comparison. From a total of about 200 possible cases, we selected 46 cases without clouds.

[35] CALIPSO level 1 data of version V2.01 are used. Attenuated backscatter profiles are provided in level 1 data with the original resolution of 1/3 km. In order to reduce the noise in the CALIPSO signal, profiles are averaged on a horizontal scale of 5 km, according to the horizontal resolution of CALIPSO level 2 aerosol layer products [Vaughan *et al.*, 2009].

[36] Figure 3 reports the mean attenuated backscatter profiles at 532 nm as measured by CALIPSO and EARLINET for the Leipzig (Figure 3a), Napoli (Figure 3b), and Potenza (Figure 3c) EARLINET stations where more data are available for this comparison; in particular, after discarding cases with low clouds in EARLINET data, 4, 21 and 11 profiles are compared with CALIPSO profiles for Leipzig, Napoli and Potenza, respectively. On average, the agreement is good demonstrating the good performance of CALIPSO and the absence of evident biases in the CALIPSO raw signals. In the mean attenuated backscatter profile measured by CALIPSO at Napoli, a low cloud at about 1.5 km is observed. No cloud clearing is applied to CALIPSO data because of our basic idea to use CALIPSO data without modifying them. For the sake of completeness, here we mention that the mean profiles and differences reported in Figure 3 do not change significantly if this case is not included. Disagreements at low altitudes are observed. Differences observed below 2 km of altitudes between EARLINET and CALIPSO can be due to different reasons, such as erroneous extinction profile needed

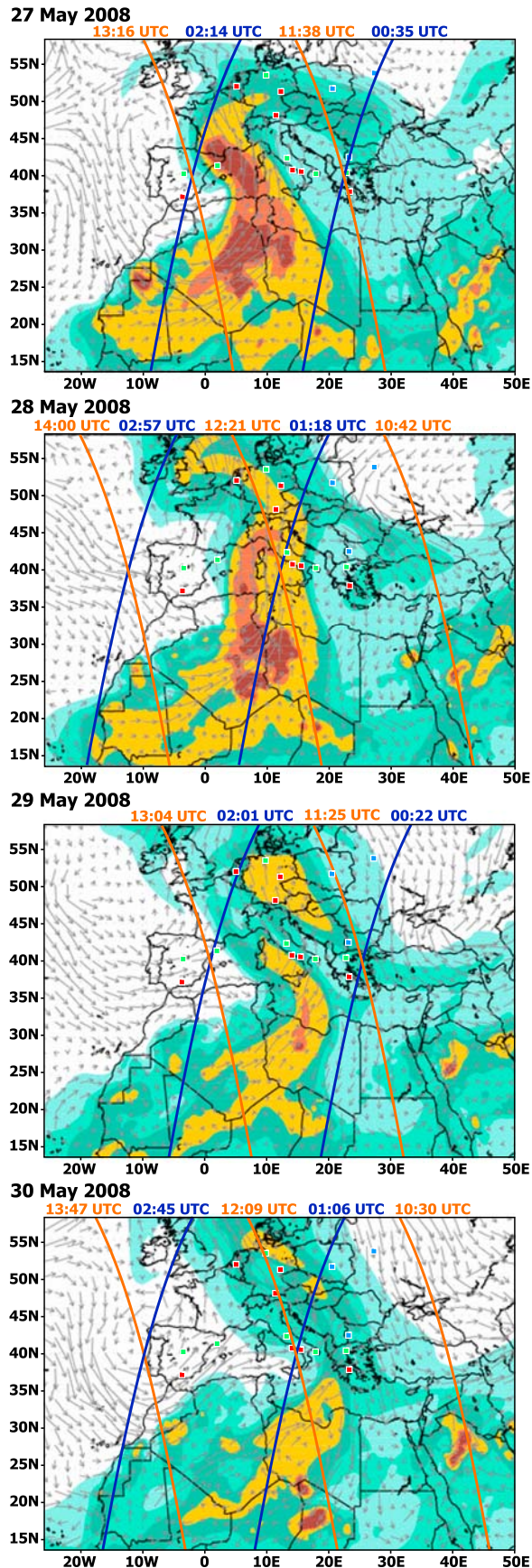
to retrieve attenuated backscatter from the ground-based observations in low altitudes and multiple scattering effects in CALIPSO data due to the presence of aerosol layer in the free troposphere. But first of all it has to be considered that horizontal distances between the two sensors in conjunction with the high variability in the aerosol content at these altitudes may lead to large differences. However, it can be seen that for Leipzig and Potenza, CALIPSO typically underestimates the effective EARLINET measurements, while for Napoli the opposite situation is found. As a consequence, there is no evidence of systematic biases for these differences observed at low altitudes.

[37] Figure 3 shows also the mean percentage differences between CALIPSO level 1 data and the corresponding attenuated backscatter profiles calculated from EARLINET measurements for each of the selected sites, Leipzig (Figure 3d), Napoli (Figure 3e), and Potenza (Figure 3f). The minimum and maximum values of these differences are reported as well. These latter values allow us to investigate the whole range of observed differences that are strongly affected by spatial and temporal variability of aerosol distribution at the different sites. On average, the agreement is good with mean values close to zero and typically within 20%.

[38] Figure 4 shows the distribution of the differences, $(\text{CALIPSO}-\text{EARLINET})/\text{EARLINET}$ (%), for all the 46 cases with data from Napoli, Leipzig, Potenza, Madrid, and Barcelona EARLINET stations, in the altitude range 1–10 km asl. Here the agreement is good as well with a relative mean difference of 4.6%, a relative standard deviation of 50% and a relative median value of 0.6%.

4.3. EARLINET Comparisons With CALIPSO Level 2 Data: 26–31 May 2008 Saharan Dust Outbreak

[39] As mentioned above, CALIPSO level 2 data consist of profile and layer products provided separately for aero-



sols and clouds. Only if a layer is clearly identified, having a certain base and a certain top height, the respective products are stored in the CALIPSO level 2 database. This evaluation scheme has several consequences for the CALIPSO data set in general and the comparison of level 2 data in particular.

[40] 1. CALIPSO extinction and backscatter profiles are generally available for identified features (i.e., profile segments) only and not as full profiles from measurement top height to ground (as the attenuated backscatter profiles). Thus level 2 profile data may consist of few data points only and the comparison of profile data is possible for certain layers only.

[41] 2. The identification of a feature and its classification by the respective CALIPSO retrieval algorithms depend on a variety of parameters such as the actual signal-to-noise ratio, the backscatter and extinction values of the feature and their gradients at the feature boundaries, the feature's optical properties (color ratio, depolarization ratio), the appearance of attenuating layers above the feature, etc. Thus level 2 data typically represent only a subset of the complete atmospheric scene covered by the cross-section curtain. Not each structure seen in the attenuated backscatter profiles is translated into level 2 data products. Furthermore, the level of identification strongly depends on daytime/nighttime conditions because of the different signal-to-noise ratio.

[42] 3. Cloud-aerosol discrimination cannot be performed perfectly. Thus misclassified cloud layers may appear in the aerosol data set and vice versa.

[43] In the following, we present a case study of a major Saharan dust outbreak. First intercomparisons of EARLINET and CALIPSO level 2 data were performed on the basis of this extended experimental data set. These intercomparisons were performed for backscatter coefficient because this is the CALIPSO level 2 product retrieved with the lowest influence of a priori assumptions. This study also illustrates the potential of correlative observations.

4.3.1. The 26–31 May 2008 Saharan Dust Outbreak

[44] In the period 26–31 May 2008 a major Saharan dust event occurred and was observed by several EARLINET stations from the Mediterranean to central and eastern Europe. This was considered as a typical case C observational period. Dust coming from the western and central Sahara was forecast over central and eastern Mediterranean and central Europe by the DREAM model for this period, and EARLINET stations were alerted accordingly.

[45] Figure 5 shows the DREAM forecast for 27–30 May, 1200 UTC, together with maps indicating the CALIPSO overpasses on these days. The major dust plume stretched from Africa over Italy toward Germany most of the time. CALIPSO crossed the central part of the dust plume during a nighttime overpass on 28 May and during a nighttime and a daytime overpass on 30 May. Case A observations for

Figure 5. DREAM forecast for 27–30 May 2008 and overlaid CALIPSO overpasses for the same days. DREAM maps show the 0 h forecast at 1200 UTC of each day in terms of column dust load (color, log scale from 0.05 to 7 g/m^2) together with the 3000 m wind field (arrows). Daytime CALIPSO overpasses are indicated in orange, and nighttime overpasses are indicated in blue. The overpass times are given above each map.

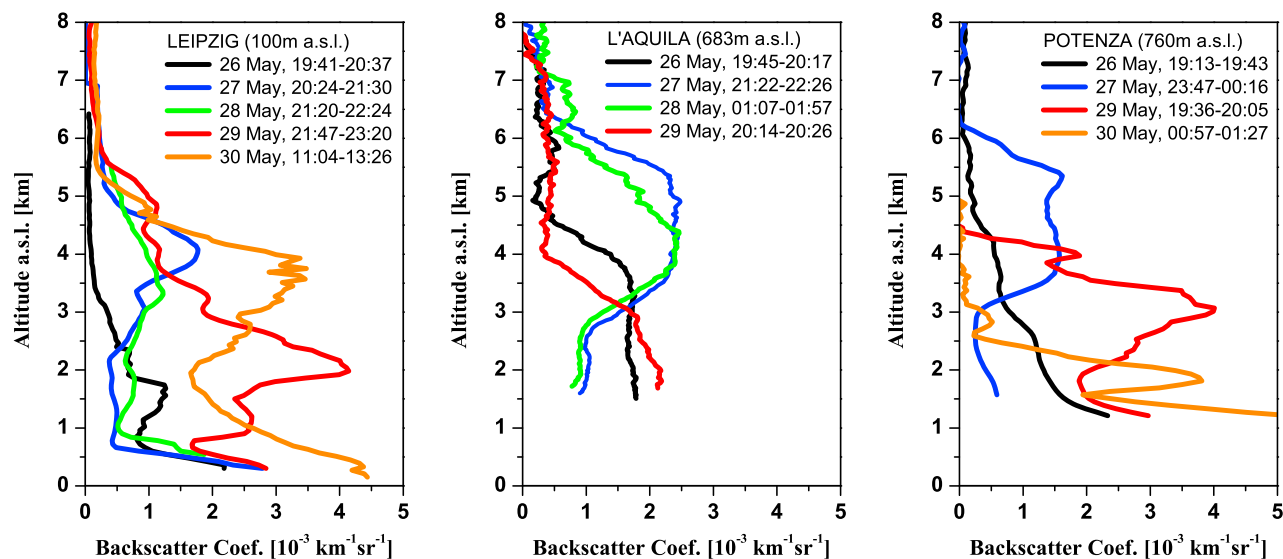


Figure 6. Backscatter coefficient profiles measured at the EARLINET stations (left) Leipzig (532 nm), (middle) L'Aquila (355 nm), and (right) Potenza (532 nm) during the major Saharan dust outbreak in the period 26–30 May 2008.

these overpasses were performed in L'Aquila on 28 May, in Belsk, Potenza, and Napoli on 30 May at night, and in Hamburg and Maisach on 30 May during daytime, together with a case B observation in Leipzig. These observations are of primary interest for level 2 intercomparisons and further discussed in section 4.3.2.

[46] Altogether, 15 case A, 7 case B, and 56 case C measurements were performed by 13 EARLINET stations in the period 26–31 May 2008. The complete data set is used to derive typical lidar ratios and Ångström exponents of the dust plume (see section 4.3.3) and in a representativeness study presented in section 5.

4.3.2. Spatial Variability and Level 2 Intercomparisons

[47] The high spatial and temporal variability of the dust plume becomes visible in the CALIPSO as well as in the EARLINET observations. Figure 6 presents a sample of backscatter coefficient profiles taken at Leipzig, L'Aquila, and Potenza, i.e., along the north-south axis of the major dust plume, from 26 to 30 May 2008. The main dust layer stretched up to 6 km height typically. Maximum backscatter coefficient values were around $0.002\text{--}0.004\text{ km}^{-1}\text{sr}^{-1}$, corresponding to extinction coefficients of $0.1\text{--}0.3\text{ km}^{-1}$. The optical depth reached values of 1–1.5 in the center of the plume, which is also confirmed by Aerosol Robotic Network (AERONET) observations at several European sites in this period.

[48] Figure 7 shows the CALIPSO cross section for the nighttime overpass on 28 May in terms of the 532 nm total attenuated backscatter and the vertical feature mask. The dust plume stretching toward Europe is circled and the location of L'Aquila EARLINET station (La) is indicated. Figure 8 shows the direct comparison of the backscatter coefficient profiles measured from ground at L'Aquila and from CALIPSO in horizontal distances of 53, 83, and 107 km. CALIPSO profiles were retrieved with an input lidar ratio of 40 sr for dust in case of the profiles at 83 and 107 km distance (see blue and black curves in Figure 8). A mean lidar ratio of 46 sr was found from the constrained

retrieval for the separated layer in the distance of 53 km (red curve). This value is in good agreement with the mean lidar ratio of $46 \pm 11\text{ sr}$ measured between 3.0 and 5.4 km height at L'Aquila.

[49] Figures 9 and 10 present a respective approach for the CALIPSO daytime overpass on 30 May. CALIPSO passed the stations of Maisach, Leipzig, and Hamburg at horizontal distances of 55 km (to the northeast), 305 km (to the west), and 20 km (to the southwest), respectively (see also Figure 5, bottom). The 532 nm total attenuated backscatter coefficient shows high and midlevel clouds over the Alps, i.e., above and south of the EARLINET station at Maisach (Ms). Cirrus clouds are also present over northern Germany (EARLINET station Hamburg, Hh). The dust plume is indicated again by a red circle in Figure 9. However, from the vertical feature mask it can be seen that most of the plume is classified as cloud. Obviously, this is a misclassification caused by the high backscatter and depolarization values of dust at relatively high latitudes. North of 50°N , outside of the so-called dust belt, the CALIPSO cloud-aerosol discrimination algorithm forces the identification of polar ice clouds instead of dust. Both features cause very similar signatures [Liu *et al.*, 2009].

[50] Measurements at Leipzig between 0900 and 1500 UTC did not show any clouds, and during the 24 h observations in Hamburg cirrus clouds above 8 km height were detected only. As a consequence of the classification, only few CALIPSO level 2 aerosol data are available for the intercomparison. One profile taken about 130 km to the north of Maisach fits quite well to the ground-based measurement at this site (see Figure 10). It can also be seen that the dust load toward the north, where the misclassification is found, was much higher, as indicated by the Leipzig and Hamburg profiles.

4.3.3. Saharan Dust Properties

[51] A complete data set from a high-performance EARLINET station is shown in Figure 11. The measurement was taken in the Saharan dust layer at Leipzig on 27

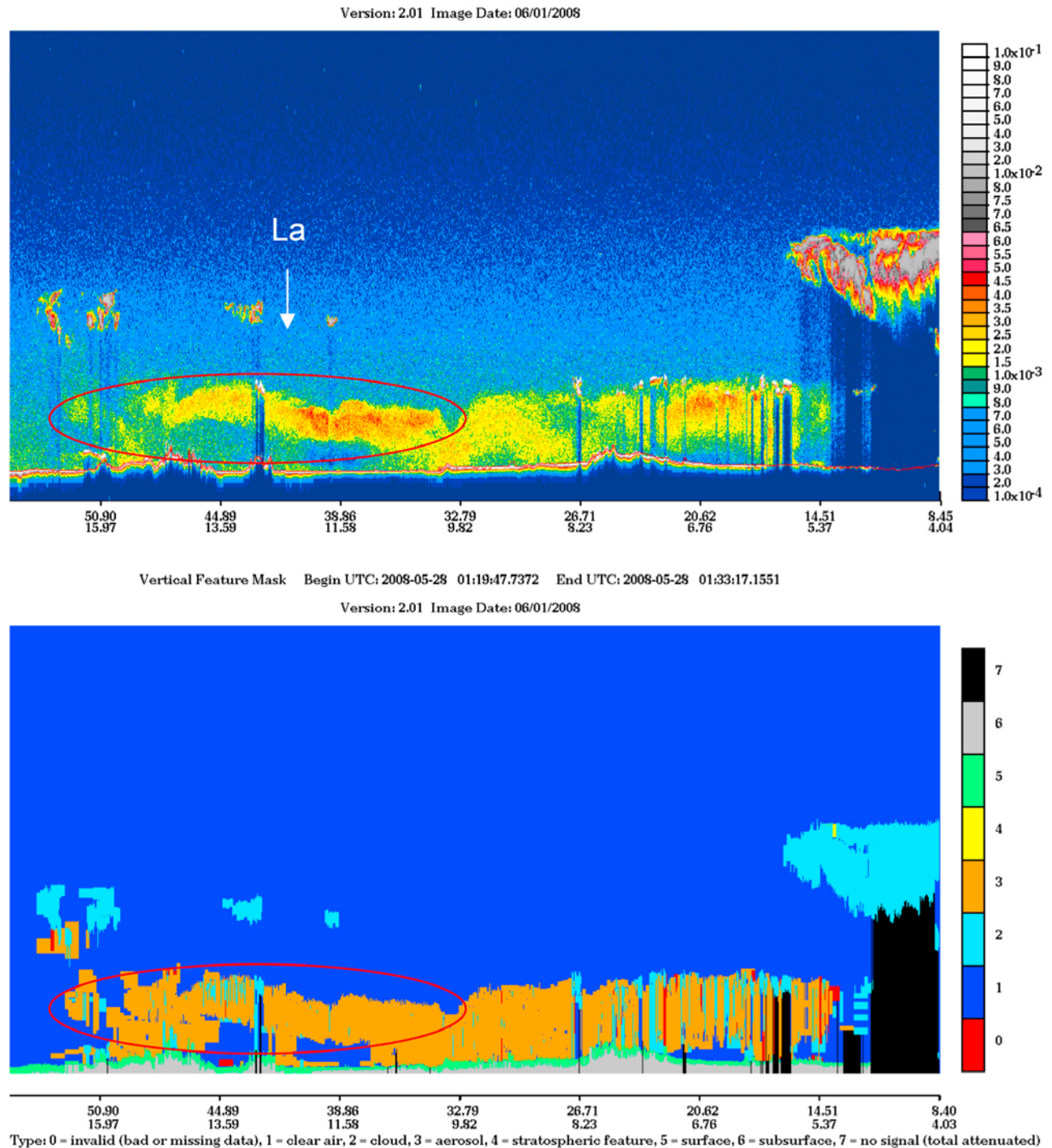


Figure 7. CALIPSO cross sections of 532 nm total attenuated backscatter and the vertical feature mask for the overpass at 0119–0133 UTC on 28 May 2008. The dust plume stretching toward central Europe is circled, and the location of L’Aquila EARLINET station is indicated. (These data were obtained from the NASA Langley Research Center Atmospheric Science Data Center, http://www-calipso.larc.nasa.gov/products/lidar/browse_images/show_calendar.php.)

May 2008, 2024–2130 UTC. Backscatter coefficients at 355, 532, and 1064 nm and extinction coefficients at 355 and 532 nm are the primary parameters derived from the lidar observations. In addition, the volume depolarization ratio at 532 nm is determined. The backscatter and extinction profiles show only a weak wavelength dependence in

the dust layer. From the primary parameters, the lidar ratios at 355 and 532 nm and the extinction-related and backscatter-related Ångström exponents are calculated. Lidar ratios around 50 sr and Ångström exponents of 0–0.5 are found. The Ångström exponents correspond to color ratios (i.e., 1064 nm/532 nm backscatter ratio, 532 nm/355 nm

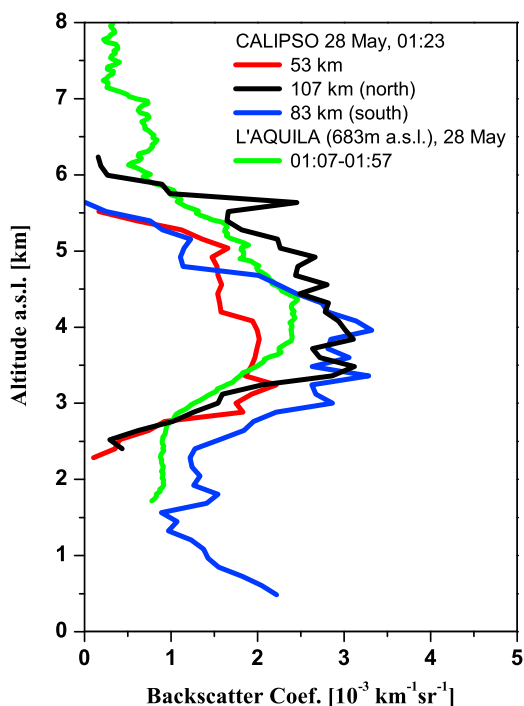


Figure 8. Backscatter coefficient profile (355 nm) taken at L'Aquila EARLINET station during the CALIPSO nighttime overpass on 28 May 2008 and corresponding backscatter coefficient profiles (532 nm) derived from CALIPSO measurements in the vicinity of L'Aquila.

backscatter ratio, and 532 nm/355 nm extinction ratio) of 0.8–1.

[52] The results of a statistical analysis of dust properties are presented in Table 2. For this investigation, we selected 44 layers, which were clearly identified as dust, from all measurements taken at the EARLINET stations of Belsk, Hamburg, L'Aquila, Leipzig, Maisach, Napoli, and Potenza in May 2008. For each layer, mean intensive optical properties (lidar ratios, Ångström exponents, color ratios) were calculated from the backscatter and extinction profiles available at the respective stations. Finally, mean values of each parameter were computed from the findings at all sites. In this way, we obtained typical lidar ratios of the dust event of 49 ± 10 sr and 56 ± 7 sr at 355 and 532 nm, respectively. The extinction-related and backscatter-related Ångström exponents were on the order of 0.15–0.17, which corresponds to respective color ratios of 0.91–0.95 (see Table 2). The mean EARLINET lidar ratio at 532 nm is significantly higher than the input lidar ratio of 40 sr used for dust in the CALIPSO retrievals. Saharan dust lidar ratios above 50 sr were found in other studies as well [Mattis *et al.*, 2002; Papayannis *et al.*, 2008; Tesche *et al.*, 2009]. The use of too low lidar ratios in the CALIPSO retrievals may lead to an underestimation of dust optical depths in general.

4.4. EARLINET-CALIPSO Long-Term Database

[53] In principle, all CALIPSO level 2 layer and profile data can be directly compared with EARLINET data for nearby overpasses (primarily case A) and stations providing data at 532 and 1064 nm. However, the potential of EARLINET as a network of multiwavelength lidar instru-

ments is much larger. As shown above, EARLINET observations allow us to investigate intensive optical parameters (i.e., lidar ratios, depolarization ratios, Ångström exponents, and color ratios) and to relate them to specific aerosol and cloud types. Such information is strongly needed as an input for the development of spaceborne lidar algorithms and their improvement. For instance, CALIPSO aerosol and cloud classification relies on predefined color ratio and depolarization ratio thresholds, and a look-up table of lidar ratios depending on aerosol and cloud type is used for extinction and backscatter retrievals. As discussed before, the distribution of stations in the network makes it possible to investigate the variability on regional and continental scales and to study the representativeness of spaceborne lidar observations.

[54] In order to make an optimal use of the complete EARLINET information not only for simple intercomparison activities but also for a sustainable support of spaceborne lidar missions in general, EARLINET and ESA have started a dedicated activity to establish a long-term aerosol and cloud database consisting of both ground-based and spaceborne lidar data. Currently, 18 months of correlative EARLINET-CALIPSO measurements are fed into the database. The EARLINET measurements are investigated in detail with respect to layer mean values of spectral backscatter and extinction coefficients, lidar ratio, depolarization ratio, extinction- and backscatter-related Ångström exponents and color ratios. Each observed cloud and aerosol layer is classified by individual inspection of the time-height contour plots of range-corrected signals and the corresponding set of mean profiles. Layer boundaries are determined from the gradient of the backscatter profile. Aerosol classification considers marine aerosol, dust, smoke, continental pollution, clean continental background aerosol, and volcanic aerosol. Extended analysis of source regions, age, and state of humidification is performed with the help of models and auxiliary data. Cloud classification focuses on the discrimination of water, ice, and mixed-phase clouds. The complete data set is stored, together with the corresponding CALIPSO level 2 layer and profile products, in a relational database which will be made available to the public in the future. Search algorithms allow for specific investigations, for example, searching for optical data by aerosol and cloud type or source region or comparing geometrical and optical layer properties measured from ground and from space. The database is designed such that it can be extended with respect to the number of stations, length of the observational period, and future spaceborne missions.

5. Representativeness Study

[55] An attempt to assess the representativeness of Sun-synchronous polar-orbiting satellite columnar measurements is reported by Kaufman *et al.* [2000]. They used ground-based aerosol optical depth measurements of AERONET to determine if measurements at a single time of the day are representative, in a climatological sense, of daily averaged measurements. In particular, the different measurements provided at one site by AERONET during one day are compared to the mean. Almost no bias and a standard deviation (therefore a variability) of about 20% were observed.

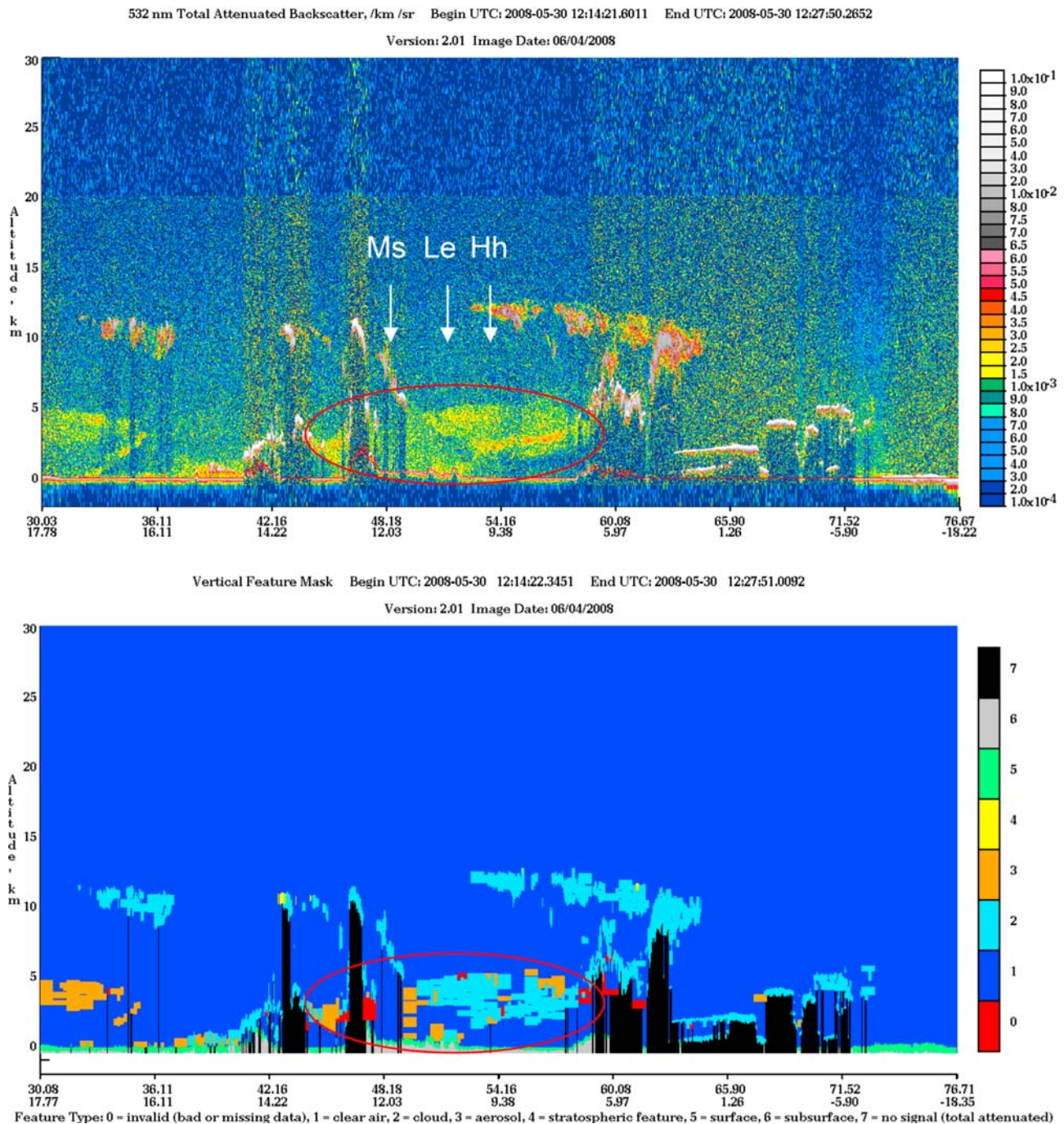


Figure 9. CALIPSO cross sections of 532 nm total attenuated backscatter and the vertical feature mask for the overpass at 1214–1227 UTC on 30 May 2008. The dust plume over central Europe is circled, and the locations of Maisach, Leipzig, and Hamburg EARLINET stations are indicated. (These data were obtained from the NASA Langley Research Center Atmospheric Science Data Center, http://www-calipso.larc.nasa.gov/products/lidar/browse_images/show_calendar.php.)

[56] Mesoscale variation of tropospheric aerosol has been extensively discussed by *Anderson et al.* [2003], starting from correlation analysis of measurements of high-resolution column-integrated optical properties. It came out that there is little variability below 20 km horizontal scale, but a sharp increase in variability is observed over horizontal scales of 20–100 km. This is mainly ascribed to major aerosol sources (like dust storms, biomass burning and anthropogenic pol-

lution) and the main sink for aerosol (precipitation) that typically are characterized by comparable horizontal extension. In this sense, aerosol plumes cover large areas but are internally not homogeneous. The main result of the study performed by *Anderson et al.* [2003] is that on scales larger than few hours or few tens of kilometers, aerosol cannot be considered as homogeneous in space and time. The authors made use of a threshold criterion on autocorrelation of 0.8 and

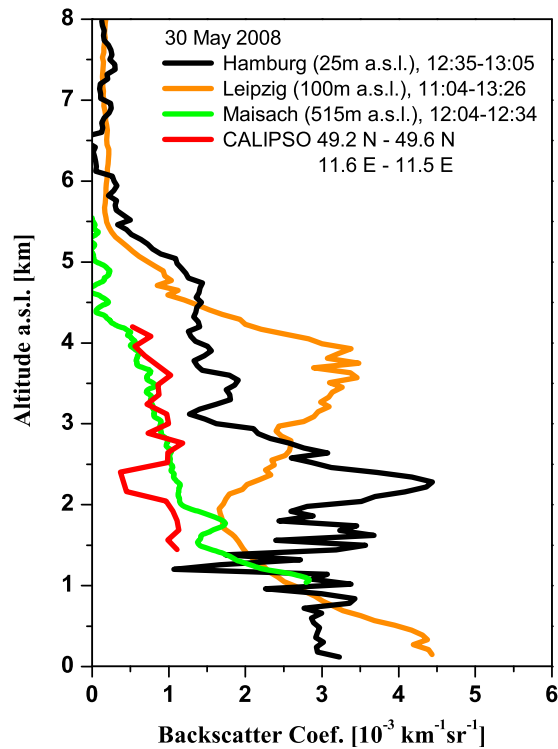


Figure 10. Backscatter coefficient profiles (532 nm) taken at the EARLINET stations Hamburg, Leipzig, and Maisach during the CALIPSO daytime overpass on 30 May 2008 and corresponding backscatter coefficient profile (532 nm) derived from CALIPSO measurements.

found that coherent time scales and space scales for aerosol columnar load are less than 10 h and 200 km, respectively. The paper highlighted the need of a statistically significant amounts of data to address representativeness. In these pre-

Table 2. Mean Properties of Saharan Dust Derived From 44 Layers Observed at Seven EARLINET Stations in May 2008

| Parameter | Mean Value and Standard Deviation |
|--|-----------------------------------|
| Lidar ratio at 355 nm | 49 ± 10 sr |
| Lidar ratio at 532 nm | 56 ± 7 sr |
| Extinction-related Ångström exponent (532 nm/355 nm) | 0.17 ± 0.2 |
| Backscatter-related Ångström exponent (532 nm/355 nm) | 0.15 ± 0.38 |
| Backscatter-related Ångström exponent (1064 nm/532 nm) | 0.15 ± 0.2 |
| Extinction-related color ratio (532 nm/355 nm) | 0.94 ± 0.08 |
| Backscatter-related color ratio (532 nm/355 nm) | 0.95 ± 0.14 |
| Backscatter-related color ratio (1064 nm/532 nm) | 0.91 ± 0.1 |

vious works, a large source of variability not considered at all is the vertical mixing, which leads to horizontal inhomogeneities due to large vertical concentration gradients.

[57] The CALIPSO mission with its high resolution both in time, and horizontal and vertical dimensions provides the first opportunity to investigate the 4-D aerosol and cloud fields in detail. The CALIPSO lidar has a small footprint and a revisiting time of 16 days, and therefore it is still an important issue to investigate how well these measurements represent the atmospheric conditions of a surrounding area over a longer time. The backbone of this representativeness study is the collection of comparisons of ground-based and satellite measurements at different temporal and spatial distances.

[58] Following the measurements strategy established for the ESA-CALIPSO study with case A, B and C measurements, the horizontal distance between CALIPSO and EARLINET selected stations covers a large interval: 0–100 km for case A (almost 60% of the cases within 50 km); 120–750 km for case B (almost 70% of the cases within

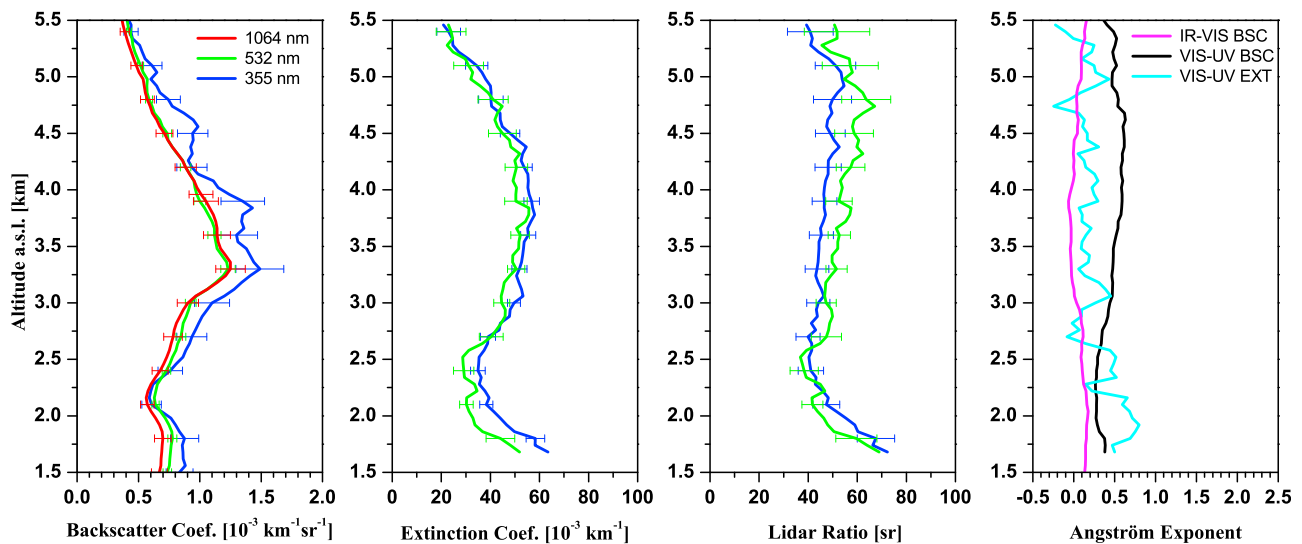


Figure 11. Observational data set of the high-performance EARLINET station at Leipzig. The measurement was taken in the Saharan dust layer on 27 May 2008, 2024–2130 UTC. Backscatter coefficients at 355, 532, and 1064 nm, extinction coefficients at 355 and 532 nm, lidar ratios at 355 and 532 nm, extinction-related Ångström exponents (532 nm/355 nm), and backscatter-related Ångström exponents (532 nm/355 nm and 1064 nm/532 nm) are derived.

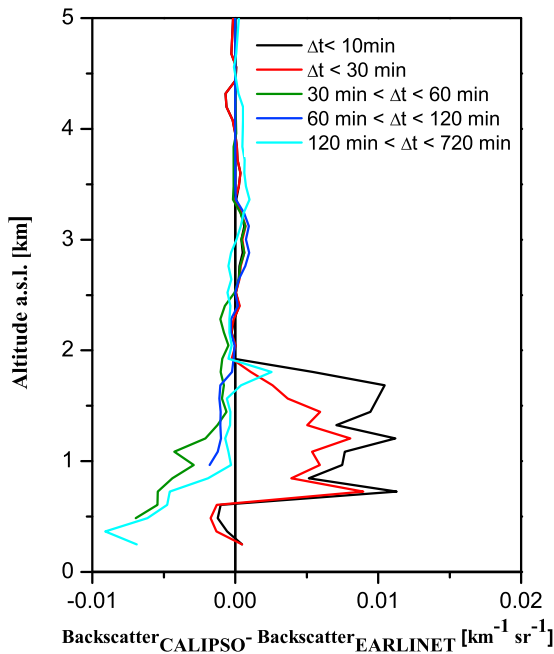


Figure 12. Mean difference profiles ($\text{Backscatter}_{\text{CALIPSO}} - \text{Backscatter}_{\text{EARLINET}}$) at 532 nm as obtained averaging over 26–31 May 2008 cases for a maximum spaceborne versus ground-based lidar horizontal distance of 100 km and for six time shift intervals (Δt).

500 km); also larger distances for case C measurements. This allows us to investigate the horizontal variability on different scales, from regional to continental. The temporal variability of aerosol/clouds fields can be investigated with the 150 min records of EARLINET measurements (centered around the overpass).

[59] Two different approaches for the representativeness study are used according to the actual strategy for the correlative measurements: (1) a point-to-point comparison, in which each EARLINET observation is compared with the corresponding CALIPSO overpass measurement; and (2) a multiple-point approach, for different scenarios such as long-range aerosol transport, in which multiple-point observations are compared with appropriate horizontal averages along the satellite cross section. In the following we report an example of this kind of representativeness study.

[60] The 26–31 May 2008 observation period has been chosen for a first correlation analysis for both single-point and multiple-point observations, because this is a period with a large number of performed measurements: 15 case A, 7 additional case B, and 56 additional case C measurements. We consider here the backscatter profiles at 532 nm, because these represent the largest number of profiles; in total 420 EARLINET files are available for this period providing a significant ground-based data set for illustrating the strategy of the representativeness study. In the backscatter comparison reported in the following, we selected EARLINET data corresponding to altitude ranges where CALIPSO reports backscatter, i.e., where an aerosol layer has been identified by CALIPSO algorithms. The comparisons of CALIPSO and EARLINET backscatter measurements at 532 nm are performed (1) for a fixed maximum horizontal distance of 100 km and different time shifts, (2) for a fixed time shift of

10 min and different horizontal distances, and (3) for different temporal and spatial distances. In total 938 CALIPSO profiles within a maximum distance of 2000 km and 12 h from EARLINET observations are selected for this study.

5.1. Comparisons for 100 km Maximum Horizontal Distance and Different Time Shifts

[61] All mean differences profiles ($\text{Backscatter}_{\text{CALIPSO}} - \text{Backscatter}_{\text{EARLINET}}$) related to a spaceborne versus ground-based lidar horizontal distance below 100 km (case A measurements) are selected and classified in classes on the base of the time shift (Δt) between the two observations, as reported in Figure 12. The mean difference profile has been calculated from 10 available difference profiles for the class $\Delta t < 10$ min, 11 for $\Delta t < 30$ min, 15 for $30 \text{ min} \leq \Delta t < 60$ min, 13 for $60 \text{ min} \leq \Delta t < 120$ min, and 26 for $120 \text{ min} \leq \Delta t < 720$ min. The largest mean differences are observed below about 2 km of altitude, with mean values of $0.008 \text{ km}^{-1} \text{ sr}^{-1}$ and $0.005 \text{ km}^{-1} \text{ sr}^{-1}$ for the 10 and 30 min time shifts, respectively, while smaller mean differences are found for larger time shifts, $-0.003 \text{ km}^{-1} \text{ sr}^{-1}$ for $30 \text{ min} \leq \Delta t < 60$ min and $-0.001 \text{ km}^{-1} \text{ sr}^{-1}$ for both $60 \text{ min} \leq \Delta t < 120$ min and $120 \text{ min} \leq \Delta t < 720$ min. In the free troposphere, above 2 km of altitude, the mean differences profiles do not change significantly with the time shifts, with values ranging between 0.00005 and $0.0001 \text{ km}^{-1} \text{ sr}^{-1}$. Below 2 km, aerosol optical properties vertical profiles are strongly dependent on time and space, because of the large variability of aerosol at these altitudes. This results in a large observed mean difference when small time shifts are considered. Smaller mean differences, observed for altitudes below 2 km and for time shifts larger than 30 min, are due to the presence of both positive and negative differences and to the large variability of the aerosol content at these altitudes, characterized by the presence of local aerosol.

[62] For a more quantitative study, we compare the count distributions of CALIPSO and EARLINET backscatter coefficient measurements for these classes with different time shifts. Figure 13 reports one example of count distribution for the backscatter coefficient measured at 532 nm by CALIPSO and EARLINET with 100 km as maximum horizontal distance and 10 min as maximum time shift between the two observations. The median values of the two data sets are in good agreement: $0.0005 \text{ km}^{-1} \text{ sr}^{-1}$ and $0.0006 \text{ km}^{-1} \text{ sr}^{-1}$ for $\text{Backscatter}_{\text{CALIPSO}}$ and $\text{Backscatter}_{\text{EARLINET}}$ observations, respectively. The agreement can be quantified through the linear correlation coefficient of the two count distributions that is 0.9 for this case. The correlation coefficient between CALIPSO and EARLINET backscatter count distributions, for spaceborne versus ground-based lidar horizontal distance below 100 km (case A measurements), remains around 0.9 for time shifts up to 30 min and decreases to 0.76 for $30 \text{ min} \leq \Delta t < 60$ min, 0.56 for $60 \text{ min} \leq \Delta t < 120$ min, 0.57 for $120 \text{ min} \leq \Delta t < 720$ min. Therefore, for time shifts larger than 30 min the two observations are not correlated, implying that on a spatial scale of 100 km the aerosol time variability for this event is on the order of 30 min.

5.2. Comparisons for 10 min Maximum Time Shift and Different Horizontal Distances

[63] While in section 5.1 the temporal variability has been investigated, here the spatial variability is studied based on

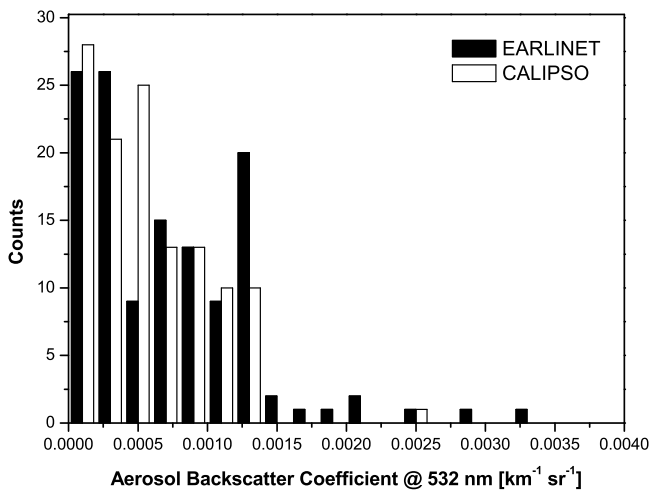


Figure 13. Count distribution of EARLINET and CALIPSO measured values of aerosol backscatter coefficient at 532 nm for spaceborne versus ground-based lidar horizontal distances lower than 100 km and 10 min for maximum time shift between the two observations.

almost simultaneous measurements (within 10 min) at different horizontal distances. Since in the investigated period, case C measurements were performed in addition to case A and case B measurements, a large data set of EARLINET measurements within 10 min and 2000 km (considered here as maximum distance for the comparisons) from the CALIPSO overpass was collected. This large data set of almost simultaneous measurements allows us to investigate the spatial variability in eight classes of horizontal distances (D): $D < 100$ km, $100 \text{ km} \leq D < 200$ km, $200 \text{ km} \leq D <$

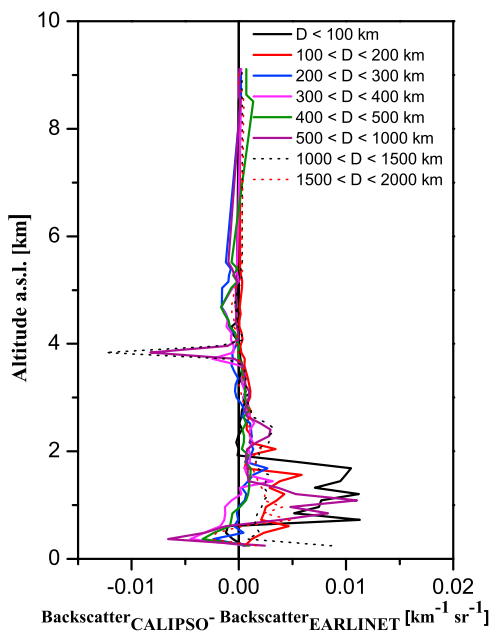


Figure 14. Mean difference profiles ($\text{Backscatter}_{\text{CALIPSO}} - \text{Backscatter}_{\text{EARLINET}}$) at 532 nm as obtained averaging over 26–31 May 2008 cases with a spaceborne versus ground-based lidar time shift lower than 10 min and for 8 horizontal distance (D) classes from 100 km up to 2000 km.

300 km, $300 \text{ km} \leq D < 400$ km, $400 \text{ km} \leq D < 500$ km, $500 \text{ km} \leq D < 1000$ km, $1000 \text{ km} \leq D < 1500$ km, and $1500 \text{ km} \leq D < 2000$ km (Figure 14). The mean difference profile has been calculated from 10 available difference profiles for the class $D < 100$ km, 20 for $100 \text{ km} \leq D < 200$ km, 34 for $200 \text{ km} \leq D < 300$ km, 23 for $300 \text{ km} \leq D < 400$ km, 25 for $400 \text{ km} \leq D < 500$ km, 103 for $500 \text{ km} \leq D < 1000$ km, 98 for $1000 \text{ km} \leq D < 1500$ km and 106 for $1500 \text{ km} \leq D < 2000$ km. In this case, as for the comparisons reported in section 5.1, the large differences observed below 2 km for smaller distance intervals are related to the high variability of aerosol at these altitudes.

[64] The linear correlation coefficient between CALIPSO counts and EARLINET counts of backscatter coefficient values is reported in Figure 15 as a function of the horizontal distance between the two observations. We observe a strong dependence on the horizontal distance with a sharp decrease of the correlation coefficient from 0.9 for a distance ≤ 100 km to 0.76 for distances between 100 and 200 km. The correlation coefficient continues to decrease with the increase of the horizontal distance between the CALIPSO and EARLINET observations.

[65] This statistical analysis performed as function of spatial and temporal differences between CALIPSO and EARLINET observations, as shown in both section 5.1 and 5.2, provides an estimate of the spatial and temporal scale of the event under study.

5.3. Comparisons for Different Time Shifts and Horizontal Distances

[66] While in sections 5.1 and 5.2 the temporal and the spatial variability have been investigated, here the strategy for studying the vertical variability is introduced. All CALIPSO and EARLINET backscatter coefficient values measured at a maximum distance of 2000 km and with time shifts ≤ 12 h between the two observations are considered here. In total we have about 75,000 backscatter values available for this comparison.

[67] Figure 16 shows count distributions of CALIPSO and EARLINET backscatter coefficient data at 532 nm for

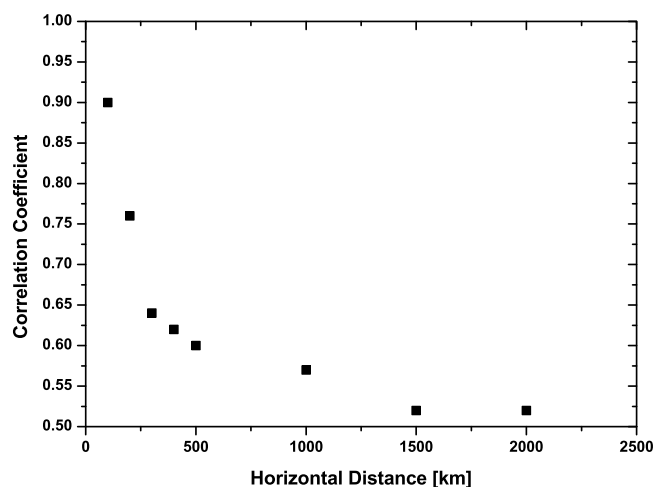


Figure 15. Correlation coefficient between CALIPSO and EARLINET backscatter count distributions for time shifts lower than 10 min reported as a function of the horizontal distance between the two observations.

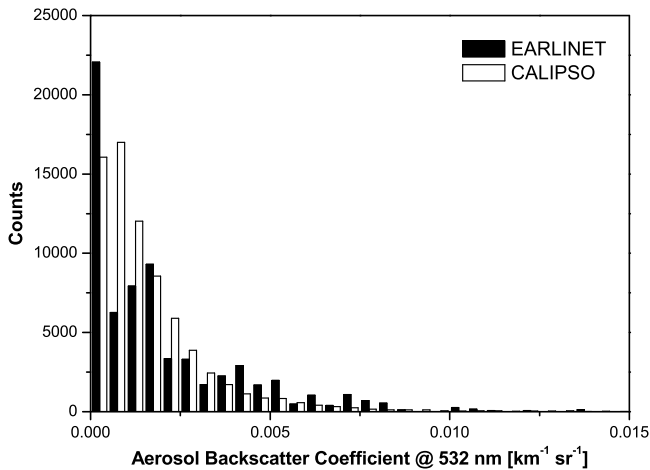


Figure 16. Count distribution of aerosol backscatter measured by CALIPSO and EARLINET within 12 h and 2000 km of distance between the two measurements.

all the available data. A good agreement is found for median values ($\text{Backscatter}_{\text{CALIPSO}} = 0.0011 \text{ km}^{-1} \text{sr}^{-1}$ and $\text{Backscatter}_{\text{EARLINET}} = 0.0012 \text{ km}^{-1} \text{sr}^{-1}$) with a reasonable correlation coefficient of 0.86.

[68] Count distributions of aerosol backscatter values measured by CALIPSO and EARLINET within 12 h and 2000 km are studied for different altitudes and reported in Figure 17 for the altitude ranges 0–1 km asl (Figure 17a), 2–3 km asl (Figure 17b), and 4–5 km asl (Figure 17c). In the first altitude range (0–1 km), the correlation between the two distributions is not very good as expected because of the more significant influence of the local boundary layer aerosol. In the altitude range 2–3 km, a much better agreement is observed with a correlation coefficient of 0.92. This result is consistent with the expected behavior of such major Saharan dust event extended on a continental scale. In the altitude range 4–5 km, we observe differences in both shape and values of the distributions. The observed differences still need to be investigated, also with view on geometrical properties of the detected layers. As mentioned before, CALIPSO level 2 profiles only report values in identified layers. Therefore, for low aerosol load some backscatter data might be missing if the layer has not been identified. On the other hand, very large aerosol load can be misclassified as clouds and excluded from the level 2 aerosol database, as demonstrated in section 4.3. Hence both of these characteristics of the CALIPSO level 2 aerosol database should be taken into account when investigating spatial and temporal variability.

[69] In the future, starting from all the available CALIPSO and EARLINET profiles, a complete analysis will allow climatological and statistical studies, in terms of geometrical and optical properties for each identified cluster of EARLINET stations, for specific scenarios (such as Saharan dust intrusions over Europe), for seasons, and for different aerosol and cloud types.

6. Summary

[70] EARLINET offers a unique opportunity for the validation and full exploitation of the CALIPSO mission. A strategy for EARLINET correlative measurements for

CALIPSO had been developed already before the launch of CALIPSO. This strategy has been consolidated in the frame of a dedicated ESA study aiming at a long-term aerosol and cloud database from ground-based and satellite-borne lidars (CALIPSO, ADM-Aeolus, and EarthCARE).

[71] EARLINET correlative measurements for CALIPSO started in June 2006 and are still in progress. Up to now more than 3100 correlative files are available on the EARLINET database.

[72] Independent extinction and backscatter measurements carried out at high-performance EARLINET stations have been used for a quantitative comparison with CALIPSO level 1 data. Results from the currently available data sets are encouraging, demonstrating the good performance of CALIPSO and the absence of evident biases in the CALIPSO raw signals.

[73] A major Saharan dust outbreak lasting from 26 to 31 May 2008 was observed from most of the EARLINET stations. The main dust layer stretched up to 6 km height typically with optical depth values of 1–1.5 in the center of the plume. In this period a large number of ground-based observations are available and for this reason this period has been used as a case study for showing first results in terms of comparison with CALIPSO level 2 data. Comparisons are good in some cases (L'Aquila and Maisach), but in other

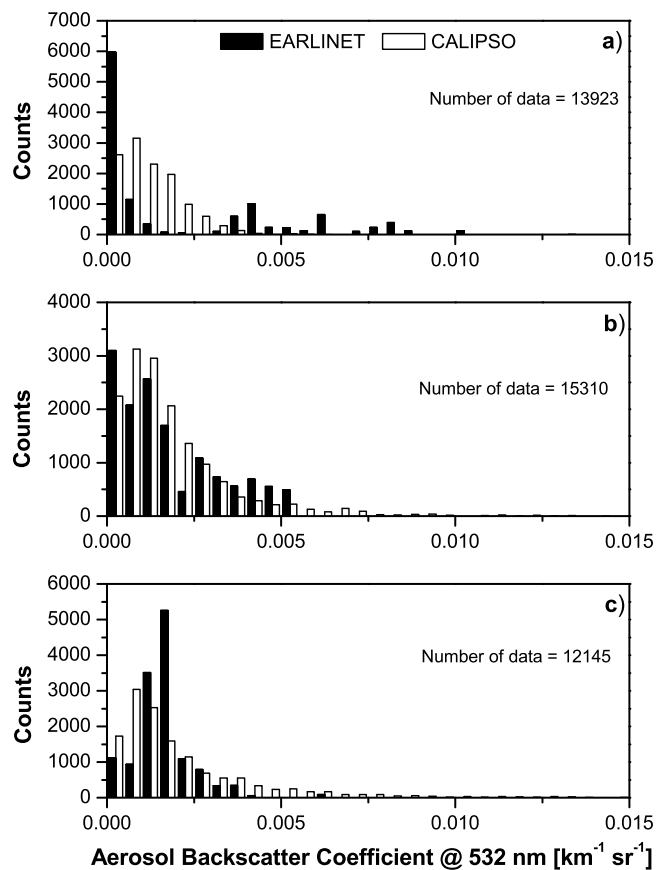


Figure 17. Count distributions of aerosol backscatter measured by CALIPSO and EARLINET within 12 h and 2000 km of distance between the two measurements for three different altitudes ranges: (a) 0–1 km, (b) 2–3 km, and (c) 4–5 km.

cases CALIPSO classifies most of the plume as cloud. Probably this misclassification is caused by the high aerosol load in conjunction with high depolarization ratios at relatively high latitudes, where a preferential identification of polar ice clouds is implemented in the CALIPSO cloud-aerosol discrimination algorithm.

[74] The large number of EARLINET observations available for this period has allowed a statistical analysis of dust properties. We observed typical lidar ratios of the dust event of 49 ± 10 sr and 56 ± 7 sr at 355 and 532 nm, respectively. The extinction-related and backscatter-related Ångström exponents were on the order of 0.15–0.17 in the 355 to 532 nm and 532 to 1064 nm ranges, which corresponds to respective color ratios of 0.91–0.95. This statistical analysis shows how EARLINET, as a network of multiwavelength lidar instruments, allows us to investigate intensive optical parameters (i.e., lidar ratios, depolarization ratios, Ångström exponents, and color ratios) and to relate these parameters to specific aerosol and cloud types. Such information is strongly needed as an input for spaceborne lidar algorithm development and improvement.

[75] The same May 2008 Saharan dust event has been used to show the methodology used for the investigation of spatial and temporal representativeness of measurements with polar-orbiting satellites. Comparisons of CALIPSO and EARLINET backscatter measurements at 532 nm have been performed for a fixed maximum distance < 100 km and different time shifts, for a fixed time shift of <10 min and different horizontal distances, and for different temporal and spatial distances. This kind of analysis performed on many different events can provide an estimate of the typical scale length for aerosol spatial and temporal variability.

[76] EARLINET correlative measurements for CALIPSO are still in progress together with the data analysis. The expected outcome from this study is a statistically significant database of correlated measurements to be used for the validation and full exploitation of the CALIPSO mission and for supporting the continuous, harmonized observation of aerosol and clouds with active remote sensing techniques from space over the next decade, including CALIPSO, ADM-Aeolus, and EarthCARE.

[77] **Acknowledgments.** The financial support for EARLINET by the European Commission under grant RICA-025991 is gratefully acknowledged. We acknowledge the support of the European Commission through GEOMon Integrated Project under the 6th Framework Programme (contract FP6-2005-Global-4-036677). The authors also acknowledge the ESA financial support under the ESTEC contract 21487/08/NL/HE and the ESRIN contract 21769/08/I-OL. CALIPSO data were obtained from the NASA Langley Research Center Atmospheric Science Data Center. The authors also thank the CALIPSO team of the NASA Langley Research Center for the provision of the CALIPSO ground track data. The atmosphere meteorological products are provided by NOAA through Real-time Environmental Applications and Display (REAL) system. We also thank the Barcelona Supercomputing Center for forecasts with the Dust Regional Atmospheric Model (DREAM). Finally, the authors want to express their thanks to Dave Winker for his stimulating suggestions.

References

Amiridis, V., D. S. Balis, S. Kazadzis, A. Bais, E. Giannakaki, A. Papayannis, and C. Zerefos (2005), Four-year aerosol observations with a Raman lidar at Thessaloniki, Greece, in the framework of European Aerosol Research Lidar Network (EARLINET), *J. Geophys. Res.*, *110*, D21203, doi:10.1029/2005JD006190.

Anderson, T. L., S. J. Masonis, D. S. Covert, N. C. Ahlquist, S. G. Howell, A. D. Clarke, and C. S. McNaughton (2003), Variability of aerosol optical properties derived from in situ aircraft measurements during ACE-Asia, *J. Geophys. Res.*, *108*(D23), 8647, doi:10.1029/2002JD003247.

Ansmann, A., and D. Müller (2005), Lidar and atmospheric aerosol particles, in *Lidar - Range-Resolved Optical Remote Sensing of the Atmosphere*, edited by C. Weitkamp, pp. 105–141, Springer, New York.

Ansmann, A., U. Wandinger, M. Riebesell, C. Weitkamp, and W. Michaelis (1992), Independent measurement of extinction and backscatter profiles in cirrus clouds by using a combined Raman elastic-backscatter lidar, *Appl. Opt.*, *31*(33), 7113–7131, doi:10.1364/AO.31.007113.

Ansmann, A., R. Neuber, P. Rairoux, and U. Wandinger (Eds.) (1997), *Advances in Atmospheric Remote Sensing With Lidar: Selected Papers of the 18th International Laser Radar Conference (ILRC)*, Springer, Berlin.

Ansmann, A., et al. (2003), Long-range transport of Saharan dust to northern Europe: The 11–16 October 2001 outbreak observed with EARLINET, *J. Geophys. Res.*, *108*(D24), 4783, doi:10.1029/2003JD003757.

Ansmann, A., U. Wandinger, O. Le Rille, D. Lajas, and A. G. Straume (2007), Particle backscatter and extinction profiling with the spaceborne HSR Doppler lidar ALADIN: Methodology and simulations, *Appl. Opt.*, *46*(26), 6606–6622, doi:10.1364/AO.46.006606.

Balis, D. S., V. Amiridis, C. Zerefos, E. Gerasopoulos, M. Andreae, P. Zanis, A. Kazantzidis, S. Kazadzis, and A. Papayannis (2003), Raman lidar and sunphotometric measurements of aerosol optical properties over Thessaloniki, Greece during a biomass burning episode, *Atmos. Environ.*, *37*(32), 4529–4538, doi:10.1016/S1352-2310(03)00581-8.

Böckmann, C., et al. (2004), Aerosol lidar intercomparison in the framework of the EARLINET project. 2. Aerosol backscatter algorithms, *Appl. Opt.*, *43*(4), 977–989, doi:10.1364/AO.43.000977.

Böckmann, C., I. Mironova, D. Müller, L. Schneidenbach, and R. Nessler (2005), Microphysical aerosol parameters from multiwavelength lidar, *J. Opt. Soc. Am. A Opt. Image Sci. Vis.*, *22*, 518–528, doi:10.1364/JO-SAA.22.000518.

Bösenberg, J., et al. (2003), EARLINET: A European Aerosol Research Lidar Network to establish an aerosol climatology, *Rep. 348*, Max-Planck-Inst. für Meteorol., Hamburg, Germany.

Damoah, R., N. Spichtinger, C. Forster, P. James, I. Mattis, U. Wandinger, S. Beirle, T. Wagner, and A. Stohl (2004), Around the world in 17 days—Hemispheric-scale transport of forest fire smoke from Russia in May 2003, *Atmos. Chem. Phys.*, *4*, 1311–1321.

De Tomasi, F., A. M. Tafuro, and M. R. Perrone (2006), Height and seasonal dependence of aerosol optical properties over southeast Italy, *J. Geophys. Res.*, *111*, D10203, doi:10.1029/2005JD006779.

Forster, C., et al. (2001), Transport of boreal forest fire emissions from Canada to Europe, *J. Geophys. Res.*, *106*, 22,887–22,906, doi:10.1029/2001JD900115.

Forster, P., et al. (2007), Changes in atmospheric constituents and in radiative forcing, in *Climate Change 2007: The Physical Science Basis. Contribution of Working Group I to the Fourth Assessment Report of the Intergovernmental Panel on Climate Change*, edited by S. Solomon et al., pp. 129–234, Cambridge Univ. Press, Cambridge, U. K.

Freudenthaler, V. (2008), The telecover test: A quality assurance tool for the optical part of a lidar system, in *Reviewed and Revised Papers Presented at 24th International Laser Radar Conference (ILRC 2008)*, edited by Organizing Committee of the 24th ILRC, pp. 145–146, Org. Comm. ILRC, Boulder, Colo.

Hélière, A., A. Lefebvre, T. Wehr, J.-L. Bézy, and Y. Durand (2008), Progress on the EarthCARE mission and its lidar instrument pre-development, in *Reviewed and Revised Papers Presented at 24th International Laser Radar Conference (ILRC 2008)*, edited by Organizing Committee of the 24th ILRC, pp. 1114–1117, Org. Comm. ILRC, Boulder, Colo.

Holben, B. N., et al. (1998), AERONET-A federated instrument network and data archive for aerosol characterization, *Remote Sens. Environ.*, *66*, 1–16, doi:10.1016/S0034-4257(98)00031-5.

Kahn, R. A., M. J. Garay, D. L. Nelson, K. K. Yau, M. A. Bull, B. J. Gaitley, J. V. Martonchik, and R. C. Levy (2007), Satellite-derived aerosol optical depth over dark water from MISR and MODIS: Comparisons with AERONET and implications for climatological studies, *J. Geophys. Res.*, *112*, D18205, doi:10.1029/2006JD008175.

Kaufman, Y. F., B. N. Holben, D. Tarré, I. Slutsker, A. Smirnov, and T. F. Eck (2000), Will aerosol measurements from Terra and Aqua polar orbiting satellites represent the daily aerosol abundance and properties?, *Geophys. Res. Lett.*, *27*, 3861–3864, doi:10.1029/2000GL011968.

Lamquin, N., C. J. Stubenrauch, and J. Pelon (2008), Upper tropospheric humidity and cirrus geometrical and optical thickness: Relationships inferred from 1 year of collocated AIRS and CALIPSO data, *J. Geophys. Res.*, *113*, D00A08, doi:10.1029/2008JD010012.

- Liu, Z., M. Vaughan, D. Winker, C. Kittaka, B. Getzewich, R. Kuehn, A. Omar, K. Powell, C. Trepte, and C. Hostetler (2009), The CALIPSO lidar cloud and aerosol discrimination: Version 2 algorithm and initial assessment of performance, *J. Atmos. Oceanic Technol.*, *26*, 1198–1213, doi:10.1175/2009JTECHA1229.1.
- Matthias, V., et al. (2004), Aerosol lidar intercomparison in the framework of the EARLINET project. 1. Instruments, *Appl. Opt.*, *43*(4), 961–976, doi:10.1364/AO.43.000961.
- Mattis, I., A. Ansmann, D. Müller, U. Wandinger, and D. Althausen (2002), Dual-wavelength Raman lidar observations of the extinction-to-backscatter ratio of Saharan dust, *Geophys. Res. Lett.*, *29*(9), 1306, doi:10.1029/2002GL014721.
- Mattis, I., A. Ansmann, U. Wandinger, and D. Müller (2003), Unexpectedly high aerosol load in the free troposphere over central Europe in spring/summer 2003, *Geophys. Res. Lett.*, *30*(22), 2178, doi:10.1029/2003GL018442.
- Mattis, I., A. Ansmann, D. Müller, U. Wandinger, and D. Althausen (2004), Multiyear aerosol observations with dual-wavelength Raman lidar in the framework of EARLINET, *J. Geophys. Res.*, *109*, D13203, doi:10.1029/2004JD004600.
- Mattis, I., D. Müller, A. Ansmann, U. Wandinger, J. Preißler, P. Seifert, and M. Tesche (2008), Ten years of multiwavelength Raman lidar observations of free-tropospheric aerosol layers over Central Europe: Geometrical properties and annual cycle, *J. Geophys. Res.*, *113*, D20202, doi:10.1029/2007JD009636.
- McCormick, M. P., et al. (1993), Scientific investigations planned for the Lidar In-space Technology Experiment (LITE), *Bull. Am. Meteorol. Soc.*, *74*, 205–214, doi:10.1175/1520-0477(1993)074<0205:SIPFTL>2.0.CO;2.
- Mona, L., A. Amodeo, M. Pandolfi, and G. Pappalardo (2006), Saharan dust intrusions in the Mediterranean area: Three years of Raman lidar measurements, *J. Geophys. Res.*, *111*, D16203, doi:10.1029/2005JD006569.
- Mona, L., G. Pappalardo, A. Amodeo, G. D'Amico, F. Madonna, A. Boselli, A. Giunta, F. Russo, and V. Cuomo (2009), One year of CNR-IMAA multi-wavelength Raman lidar measurements in correspondence of CALIPSO overpass: Level 1 products comparison, *Atmos. Chem. Phys.*, *9*, 7213–7228.
- Müller, D., U. Wandinger, D. Althausen, and M. Fiebig (2001), Comprehensive particle characterization from 3-wavelength Raman-lidar observations: Case study, *Appl. Opt.*, *40*(27), 4863–4869, doi:10.1364/AO.40.004863.
- Müller, D., A. Ansmann, I. Mattis, M. Tesche, U. Wandinger, D. Althausen, and G. Pisani (2007a), Aerosol-type-dependent lidar ratios observed with Raman lidar, *J. Geophys. Res.*, *112*, D16202, doi:10.1029/2006JD008292.
- Müller, D., I. Mattis, A. Ansmann, U. Wandinger, C. Ritter, and D. Kaiser (2007b), Multiwavelength Raman lidar observations of particle growth during long-range transport of forest-fire smoke in the free troposphere, *Geophys. Res. Lett.*, *34*, L05803, doi:10.1029/2006GL027936.
- Nickovic, S., A. Papadopoulos, O. Kakaliagou, and G. Kallos (2001), Model for prediction of desert dust cycle in the atmosphere, *J. Geophys. Res.*, *106*, 18,113–18,129, doi:10.1029/2000JD900794.
- Omar, A. H., J. G. Won, D. M. Winker, S.-C. Yoon, O. Dubovik, and M. P. McCormick (2005), Development of global aerosol models using cluster analysis of Aerosol Robotic Network (AERONET) measurements, *J. Geophys. Res.*, *110*, D10S14, doi:10.1029/2004JD004874.
- Papayannis, A., D. Balis, V. Amiridis, G. Chourdakis, G. Tsaknakis, C. Zerefos, A. D. A. Castanho, S. Nickovic, S. Kazadzis, and J. Grabowski (2005), Measurements of Saharan dust aerosols over the eastern Mediterranean using elastic backscatter-Raman lidar, spectrophotometric and satellite observations in the frame of the EARLINET project, *Atmos. Chem. Phys.*, *5*, 2065–2079.
- Papayannis, A., et al. (2008), Systematic lidar observations of Saharan dust over Europe in the frame of EARLINET (2000–2002), *J. Geophys. Res.*, *113*, D10204, doi:10.1029/2007JD009028.
- Pappalardo, G., A. Amodeo, L. Mona, M. Pandolfi, N. Pergola, and V. Cuomo (2004a), Raman lidar observations of aerosol emitted during the 2002 Etna eruption, *Geophys. Res. Lett.*, *31*, L05120, doi:10.1029/2003GL019073.
- Pappalardo, G., et al. (2004b), Aerosol lidar intercomparison in the framework of the EARLINET project. 3. Raman lidar algorithm for aerosol extinction, backscatter and lidar ratio, *Appl. Opt.*, *43*(28), 5370–5385, doi:10.1364/AO.43.005370.
- Powell, K. A., et al. (2009), CALIPSO lidar calibration algorithms: Part I-Nighttime 532-nm parallel channel and 532-nm perpendicular channel, *J. Atmos. Oceanic Technol.*, *26*, 2015–2033, doi:10.1175/2009JTECHA1242.1.
- Seifert, P., R. Engelmann, A. Ansmann, U. Wandinger, I. Mattis, D. Althausen, and J. Fruntke (2008), Characterization of specular reflections in mixed-phase and ice clouds based on scanning, polarization, and Raman lidar, in *Reviewed and Revised Papers Presented at 24th International Laser Radar Conference (ILRC 2008)*, edited by Organizing Committee of the 24th ILRC, pp. 571–574, Org. Comm. ILRC, Boulder, Colo.
- Stoffelen, A., et al. (2005), The Atmospheric Dynamics Mission for global wind field measurement, *Bull. Am. Meteorol. Soc.*, *86*, 73–87, doi:10.1175/BAMS-86-1-73.
- Stohl, A., and D. J. Thomson (1999), A density correction for Lagrangian particle dispersion models, *Boundary Layer Meteorol.*, *90*, 155–167, doi:10.1023/A:1001741110696.
- Stohl, A., M. Hittenberger, and G. Wotawa (1998), Validation of the Lagrangian particle dispersion model FLEXPART against large scale tracer experiment data, *Atmos. Environ.*, *32*(24), 4245–4264, doi:10.1016/S1352-2310(98)00184-8.
- Tesche, M., et al. (2009), Vertical profiling of Saharan dust with Raman lidar and airborne HSRL in southern Morocco during SAMUM, *Tellus, Ser. B*, *61*, 144–164, doi:10.1111/j.1600-0889.2008.00390.x.
- Vaughan, M., K. Powell, R. Kuehn, S. Young, D. Winker, C. Hostetler, W. Hunt, Z. Liu, M. McGill, and B. Getzewich (2009), Fully automated detection of cloud and aerosol layers in the CALIPSO lidar measurements, *J. Atmos. Oceanic Technol.*, *26*, 2034–2050, doi:10.1175/2009JTECHA1228.1.
- Veselovskii, I., A. Kolgotin, V. Griaznov, D. Muller, U. Wandinger, and D. N. Whiteman (2002), Inversion with regularization for the retrieval of tropospheric aerosol parameters from multiwavelength lidar sounding, *Appl. Opt.*, *41*(18), 3685–3699, doi:10.1364/AO.41.003685.
- Wandinger, U., et al. (2004), Air-mass modification over Europe: EARLINET aerosol observations from Wales to Belarus, *J. Geophys. Res.*, *109*, D24205, doi:10.1029/2004JD005142.
- Wiegner, M., S. Emes, V. Freudenthaler, B. Heese, W. Junkermann, C. Münkel, K. Schäfer, M. Seefeldner, and S. Vogt (2006), Mixing layer height over Munich, Germany: Variability and comparisons of different methodologies, *J. Geophys. Res.*, *111*, D13201, doi:10.1029/2005JD006593.
- Winker, D. (2003), Accounting for multiple scattering in retrievals from space lidar, *Proc. SPIE Int. Soc. Opt. Eng.*, *5059*, 128–139.
- Winker, D., C. Trepte, J. Pelon, A. Garnier, and T. Kovacs (2004), CALIOP Science Validation Plan, *Rep. PC-SCI-501*, Hampton Univ., Hampton, Va. (Available at <http://calipsovalidation.hamptonu.edu/misionplan.htm>)
- Winker, D. M., W. H. Hunt, and M. J. McGill (2007), Initial performance assessment of CALIOP, *Geophys. Res. Lett.*, *34*, L19803, doi:10.1029/2007GL030135.
- Winker, D. M., M. A. Vaughan, A. Omar, Y. Hu, K. A. Powell, Z. Liu, W. H. Hunt, and S. A. Young (2009), Overview of the CALIPSO mission and CALIOP data processing algorithms, *J. Atmos. Oceanic Technol.*, *26*, 2310–2323, doi:10.1175/2009JTECHA1281.1.
- Young, S. A., and M. A. Vaughan (2009), The retrieval of profiles of particulate extinction from Cloud-Aerosol Lidar Infrared Pathfinder Satellite Observations (CALIPSO) data: Algorithm description, *J. Atmos. Oceanic Technol.*, *26*, 1105–1119, doi:10.1175/2008JTECHA1221.1.

L. Alados Arboledas, Universidad de Granada, Avda. del Hospicio, E-18071 Granada, Spain.

A. Amodeo, G. D'Amico, A. Giunta, F. Madonna, L. Mona, G. Pappalardo, and F. Russo, Istituto di Metodologie per l'Analisi Ambientale, IMAA, CNR, Contrada S. Loja, Tito Salo, I-85050 Potenza, Italy. (pappalardo@imaa.cnr.it)

A. Ansmann, A. Hiebsch, I. Mattis, P. Seifert, and U. Wandinger, Leibniz-Institut für Troposphärenforschung, Permoserstr. 15, D-04318 Leipzig, Germany.

A. Apituley, Rijksinstituut voor Volksgezondheid en Milieu, Antonie van Leeuwenhoeklaan 9, NL-3721 MA Bilthoven, Netherlands.

D. Balis and E. Giannakaki, Aristotle University of Thessaloniki, GR-54124 Thessaloniki, Greece.

A. Chaikovskiy, Institute of Physics, National Academy of Sciences, 66 Independence Ave., Minsk, BY-220072, Belarus.

F. De Tomasi, Department of Physics, Università del Salento, Piazza Tancredi, N.7, I-73100 Lecce, Italy.

V. Freudenthaler, F. Schnell, and M. Wiegner, Ludwig-Maximilians-Universität, D-80539 München, Germany.

I. Grigorov, Institute of Electronics, Bulgarian Academy of Sciences, 1784 Sofia, Bulgaria.

M. Iarlori and V. Rizi, CETEMPS, Dipartimento di Fisica, Università degli Studi dell'Aquila, I-67100 L'Aquila, Italy.

H. Linné, Max-Planck-Institut für Meteorologie, Bundesstr. 55, D-20146 Hamburg, Germany.

R.-E. Mamouri and A. Papayannis, Department of Physics, National Technical University of Athens, Zografou Campus, GR-15780 Athens, Greece.

L. Nasti, N. Spinelli, and X. Wang, Consorzio Nazionale Interuniversitario per le Scienze Fisiche della Materia, I-80126, Napoli, Italy.

A. Pietruczuk, Institute of Geophysics, Polish Academy of Sciences, 01-452 Warsaw, Poland.

M. Pujadas, Centro de Investigaciones Energéticas, Medioambientales y Tecnológicas, Avda. Complutense 22, E-28040 Madrid, Spain.

F. Rocadenbosch, IEEC, CRAE, Universitat Politècnica de Catalunya, E-08034 Barcelona, Spain.